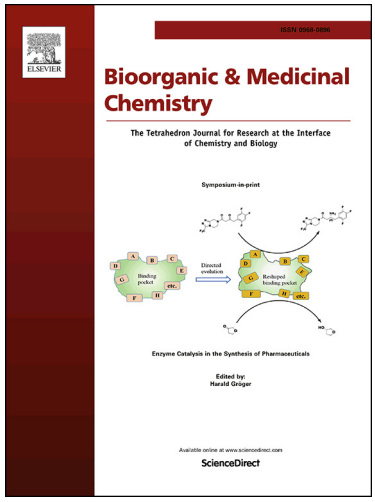

1*H*-pyrrolo[2,3-*b*]pyridine: a new scaffold for human neutrophil elastase (HNE) inhibitors

Letizia Crocetti, Maria Paola Giovannoni, Igor A. Schepetkin, Mark T. Quinn, Andrei I. Khlebnikov, Niccolò Cantini, Gabriella Guerrini, Antonella Iacovone, Elisabetta Teodori, Claudia Vergelli

PII: S0968-0896(18)31211-2
DOI: https://doi.org/10.1016/j.bmc.2018.09.034
Reference: BMC 14559

To appear in: *Bioorganic & Medicinal Chemistry*

Received Date: 11 July 2018
Revised Date: 20 September 2018
Accepted Date: 26 September 2018

Please cite this article as: Crocetti, L., Giovannoni, M.P., Schepetkin, I.A., Quinn, M.T., Khlebnikov, A.I., Cantini, N., Guerrini, G., Iacovone, A., Teodori, E., Vergelli, C., 1*H*-pyrrolo[2,3-*b*]pyridine: a new scaffold for human neutrophil elastase (HNE) inhibitors, *Bioorganic & Medicinal Chemistry* (2018), doi: https://doi.org/10.1016/j.bmc.2018.09.034

1*H*-pyrrolo[2,3-*b*]pyridine: a new scaffold for human neutrophil elastase (HNE) inhibitors

Letizia Crocetti[a], Maria Paola Giovannoni[a], Igor A. Schepetkin[b], Mark T. Quinn[b], Andrei I. Khlebnikov[c,d], Niccolò Cantini[a], Gabriella Guerrini[a], Antonella Iacovone[a], Elisabetta Teodori[a], Claudia Vergelli[a]*

[a]NEUROFARBA, Pharmaceutical and Nutraceutical Section, University of Florence, Via Ugo Schiff 6, 50019 Sesto Fiorentino, Italy.

[b]Department of Microbiology and Immunology, Montana State University, Bozeman, MT 59717, USA.

[c]Kizhner Research Center, Tomsk Polytechnic University, Tomsk 634050, Russia.

[d]Department of Chemistry, Altai State Technical University, Barnaul 656038, Russia.

[*]**Corresponding Author**

Maria Paola Giovannoni
Dipartimento di NEUROFARBA
Via Ugo Schiff 6
Sesto Fiorentino 50019 Firenze
Tel +39-055-4573683
E-mail mariapaola.giovannoni@unifi.it

Abstract

Human neutrophil elastase (HNE) is a potent serine protease belonging to the chymotrypsin family. It is an important target for the development of novel and selective inhibitors for the treatment of inflammatory diseases, especially pulmonary pathologies. Here, we report the synthesis and biological evaluation of a new series of HNE inhibitors with a pyrrolo[2,3-*b*]pyridine scaffold, which is an isomer of our previously reported indazoles, in order to assess how shift of the nitrogen from position 2 to position 7 influences activity. The majority of new compounds were effective HNE inhibitors and had IC_{50} values in the micromolar/submicromolar range, with some compounds active in low nanomolar levels. For example, **2a** and **2b** inhibited HNE with IC_{50} values of 15 and 14 nM, respectively. Molecular modeling of compounds differing in the position of heteroatom(s) in

the bicyclic moiety and in the oxadiazole ring demonstrated that the calculated geometries of enzyme-inhibitor complexes were in agreement with the observed biological activities. Docking experiments showed that orientation of the active pyrrolo[2,3-*b*]pyridines in the HNE catalytic triad Ser195-His57-Asp102 correlated with effectiveness of the inhibitor interaction with the enzyme. Thus, the pyrrolo[2,3-*b*]pyridine scaffold represents a novel scaffold for the development of potent HNE inhibitors.

Keywords: human neutrophil elastase, inhibitor, pyrrolo[2,3-b]pyridine, molecular docking.

1. Introduction

In many respiratory diseases that are characterized by an intense inflammatory component, such as chronic obstructive pulmonary disease (COPD), cystic fibrosis, bronchiectasis, acute lung injury (ALI), and acute respiratory distress syndrome (ARDS), a local imbalance occurs between proteases (serine proteases, cathepsins, metalloproteases) and anti-proteases (alpha1-antitrypsin [α1-AT], α2-macroglobulin, cystatins, tissue inhibitors of metalloproteases). The pro-inflammatory imbalance is usually associated with tissue damage and systemic involvement[1,2]. A key mediator of neutrophil-driven inflammation is human neutrophil elastase (HNE), which belongs to the chymotrypsin family of serine proteases. HNE is stored in neutrophil azurophil granules and is released upon neutrophil activation during many physiological processes, such as inflammation, immune responses, apoptosis, and tissue homeostasis[3]. Excessive HNE activity is implicated in the development of a variety of diseases, especially those affecting the respiratory system. However, recent studies have shown that HNE also participates in the progression of various types of cancer[4,5] and in other inflammatory diseases, such as rheumatoid arthritis[6]. Thus, agents able to modulate HNE proteolytic activity could represent promising therapeutics, as suggested by the interest from pharmaceutical industries[7-9].

Currently, two HNE inhibitors are commercially available: Sivelestat (Elaspol® 100, **Figure 1**), which is a non-peptide small-molecule HNE inhibitor used for the treatment of ALI and ARDS and is marketed only in Korea and Japan[10] and Prolastin (purified α1-AT),

which is used for the treatment of α1-antitrypsin deficiency[11]. Additionally, Alvelestat (AZD9668, Astra Zeneca, Cambridge, Germany)[12] and BAY 85-8501 (Bayer HealthCare, Leverkusen, Germany)[13] (**Figure 1**) are currently in clinical trials (Phase II) for patients with bronchiectasis, COPD, and cystic fibrosis.

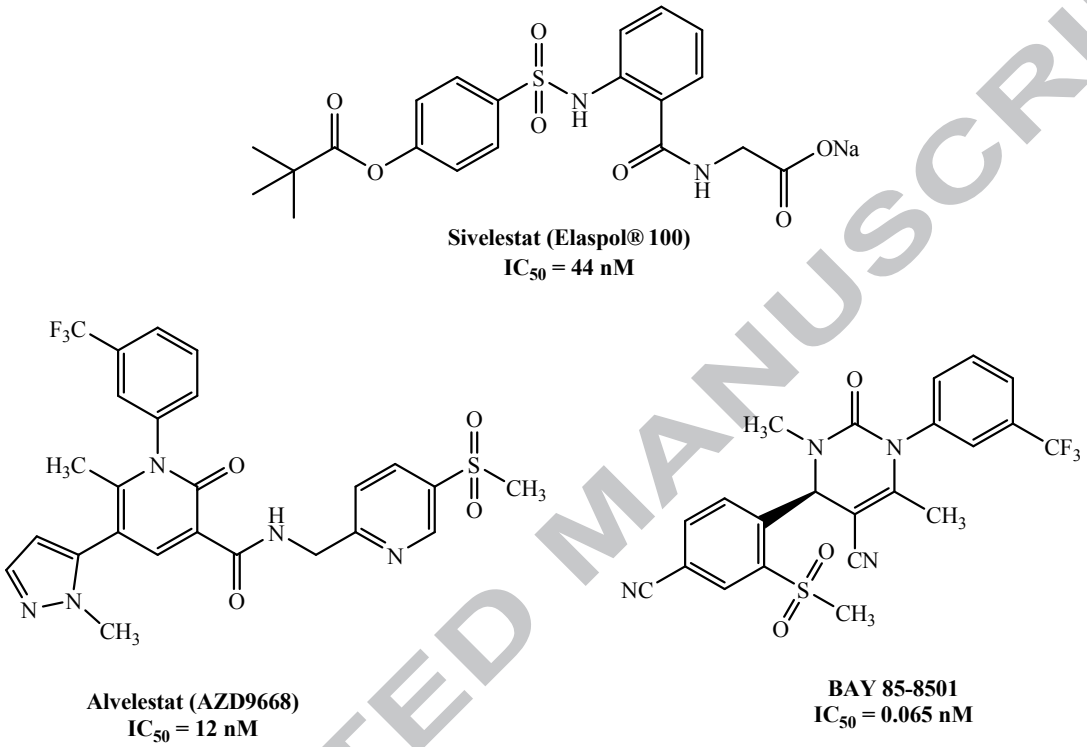

Figure 1. Current HNE inhibitors commercially available or in clinical trials.

Our previous research on the design and the synthesis of small-molecule HNE inhibitors has focused on several nitrogen bicyclic scaffolds, such as the indazole[14,15], indole[16], and cinnoline[17] scaffolds. Recently, we reported that compounds with an isoxazolone monocyclic nucleus[18,19] were effective HNE inhibitors. The most potent compounds were a series of *N*-benzoylindazoles, which had activity in the nanomolar range (IC_{50} = 7-80 nM)[15] (**Figure 2**, compounds **A**). Analysis of these compounds using molecular modeling highlighted the importance of an amidic function at position 1 as a point of attack for Ser195 and the presence of an H-bond between the nitrogen at position 2 and Gly193, which is responsible for correct anchoring in the enzyme pocket. These data were supported by the inactivity of indazole derivatives lacking the N-CO function at position 1, as well as by the low activity/inactivity of a series of indole derivatives lacking the nitrogen at position 2 (**Figure 2**, compound **B**)[16].

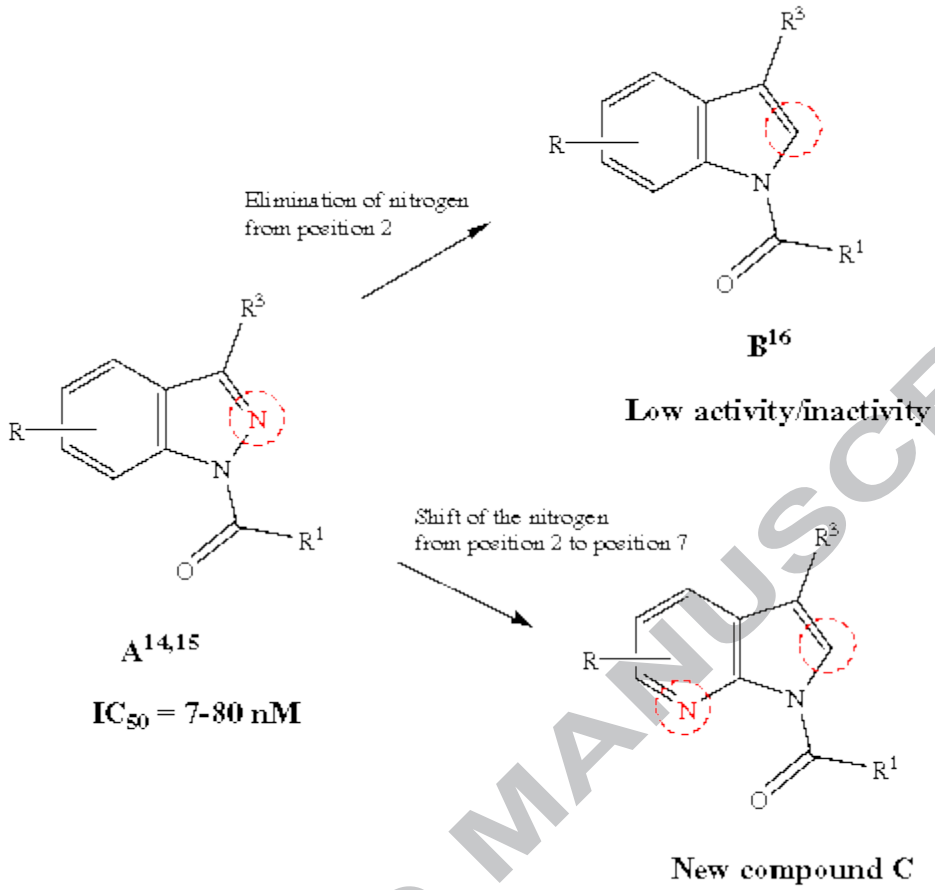

Figure 2. Design of 7-azaindole (**C**) derivatives based on the indazole (**A**) and indole (**B**) scaffolds of our previous HNE inhibitors.

Considering these requirements, we investigated the pyrrolo[2,3-*b*]pyridine scaffold (7-azaindoles) as an isomer of the indazoles described above in order to assess how a shift of the nitrogen from position 2 to position 7 influences inhibitory activity (**Figure 2**, compounds **C**). Here, we report the synthesis and the biological evaluation of this new series of pyrrolo[2,3-*b*]pyridines modified at position N1 and C3 with those substituents that gave the best results in our previous series studies, as well as with the addition of new groups and functions.

2. Results and discussion

2.1. Chemistry

All of the new compounds were synthesized as reported in **Schemes 1-6**, and the structures were confirmed on the basis of analytical and spectral data. **Scheme 1** shows the synthetic pathway leading to the 1,3-disubstituted-7-azaindoles of type **2-5**. The suitable 3-substituted intermediates **1a-h**[20-26] were reacted with the appropriate acyl or aroyl chloride

and Et_3N in anhydrous dichloromethane, resulting in compounds **2-5** (**2j**[26]), with the exception of compounds **2m**, **3f**, and **4c**, which were obtained using the appropriate halide derivatives in anhydrous acetonitrile and K_2CO_3 at reflux.

SCHEME 1[a]

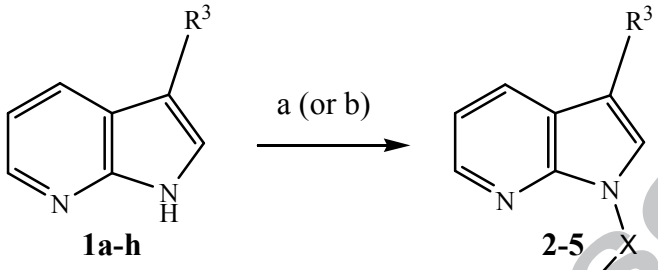

1a-h **2-5**

Compd.	R^3	X	R^1
2a	CN	CO	m-CH_3-Ph
2b	CN	CO	p-CH_3-Ph
2c	CN	CO	m-CN-Ph
2d	CN	CO	p-CN-Ph
2e	CN	CO	m-CF_3-Ph
2f	CN	CO	p-CF_3-Ph
2g	CN	CO	cC_3H_5
2h	CN	CO	cC_5H_9
2i	CN	CO	cC_6H_{11}
2j	CN	CO	CH_3
2k	CN	CO	nC_3H_7
2l	CN	CO	nC_4H_9
2m	CN	CH_2CONH	Ph
3a	COOEt	CO	m-CH_3-Ph
3b	COOEt	CO	p-CH_3-Ph
3c	COOEt	CO	m-CN-Ph
3d	COOEt	CO	p-CN-Ph
3e	COOEt	CO	cC_3H_5
3f	COOEt	CH_2CONH	Ph
4a	CONHPh	CO	m-CH_3-Ph
4b	CONHPh	CO	cC_3H_5
4c	CONHPh	-	CH_3
5a	H	CO	m-CH_3-Ph
5b	Cl	CO	m-CH_3-Ph
5c	Br	CO	m-CH_3-Ph
5d	I	CO	m-CH_3-Ph
5e	NO_2	CO	m-CH_3-Ph

Compd.	R^3
1a	CN
1b	COOEt
1c	CONHPh
1d	H
1e	Cl
1f	Br
1g	I
1h	NO_2

[a]**Reactions and conditions: a) acylation:** R^1-COCl, anhydrous CH_2Cl_2, Et_3N, 0°C, 2 h then r.t., 2 h; **b) alkylation (for compounds 2m, 3f and 4c):** R^1-Cl, anhydrous CH_3CN, K_2CO_3, reflux, 7 h.

Scheme 2 shows the synthetic route leading to the azaindole derivatives **10a** and **11**. In the first step, a reductive amination on the formyl intermediate **6**[27] using *N*-methyl aniline (compound **7a**) or aniline (compound **7b**) and $NaBH(OAc)_3$ in anhydrous dichloromethane was performed. To obtain **10a**, we removed the benzensulfonyl fragment at N1 with tetrabutylammonium fluoride in dry tetrahydrofuran (intermediate **9a**) and then performed the final benzoylation (**10a**) under the same conditions as described in **Scheme 1**. For synthesis of **11**, it was necessary to protect the aniline NH with allyl chloroformate (**8**), remove the benzensulfonyl fragment (**9b**), insert the m-toluoyl group at N1 (**10b**), and finally deprotect the aniline NH with tetrakis(triphenylphosphine)palladium(0) and phenylsilane in dry dichloromethane.

SCHEME 2[a]

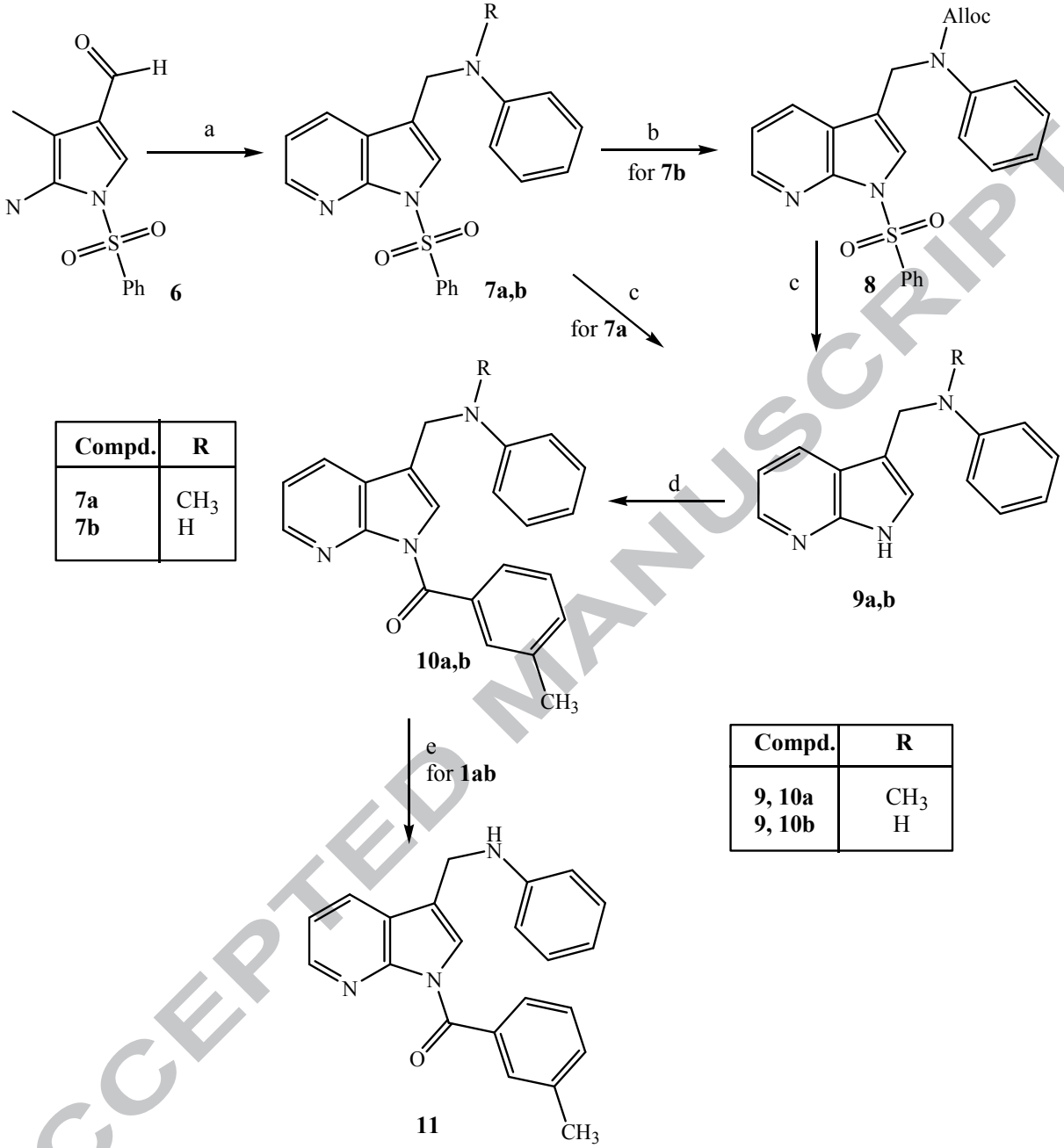

Compd.	R
7a	CH_3
7b	H

Compd.	R
9, 10a	CH_3
9, 10b	H

[a]**Reactions and conditions: a)** Aniline or *N*-methylaniline, anhydrous CH_2Cl_2, CH_3COOH, $NaBH(OAc)_3$, r.t., 24 h; **b)** NaN_3, allyl chloroformate, dioxane, r.t., 1 h, then intermediate **7b**, Na_2CO_3 1% solution, dioxane , r.t., 24 h; **c)** TBAF, anhydrous THF, reflux, 3 h; **d)** m-toluoyl chloride, anhydrous CH_2Cl_2, 0 °C, 2h, then r.t., 2 h; **e)** phenylsilane, tetrakis(triphenylphosphine)palladium(0), anhydrous CH_2Cl_2, r.t., 1 h.

Scheme 3 shows the synthesis of the two isomers **14** and **18**, both containing an oxadiazole ring as bioisoster of the carbethoxy group at position 3, but differently connected. Starting from the 7-azaindole-3-carbonitrile **1a**[20], treatment with hydroxylamine hydrochloride led to the intermediate **12**[28], which was then cyclized with dicyclohexylcarbodiimide (DCC) and acetic acid in dry DMF, resulting in 5-methyl-3-(1*H*-pyrrolo[2,3-*b*]pyridine-3-yl)-1,2,4-oxadiazole (**13**). The final acylation with m-toluoyl chloride and Et_3N in anhydrous

dichloromethane led to **14**. Alternatively, starting from the 7-azaindole-3-carboxamide **15**[29], treatment with *N,N*-dimethylacetamide dimethyl acetal in toluene at reflux (compound **16**), followed by the cyclization with hydroxylamine hydrochloride, resulted in the oxadiazole **17**. The final compound **18** was then obtained through the benzoylation at N1 following the same procedure as described above.

SCHEME 3[a]

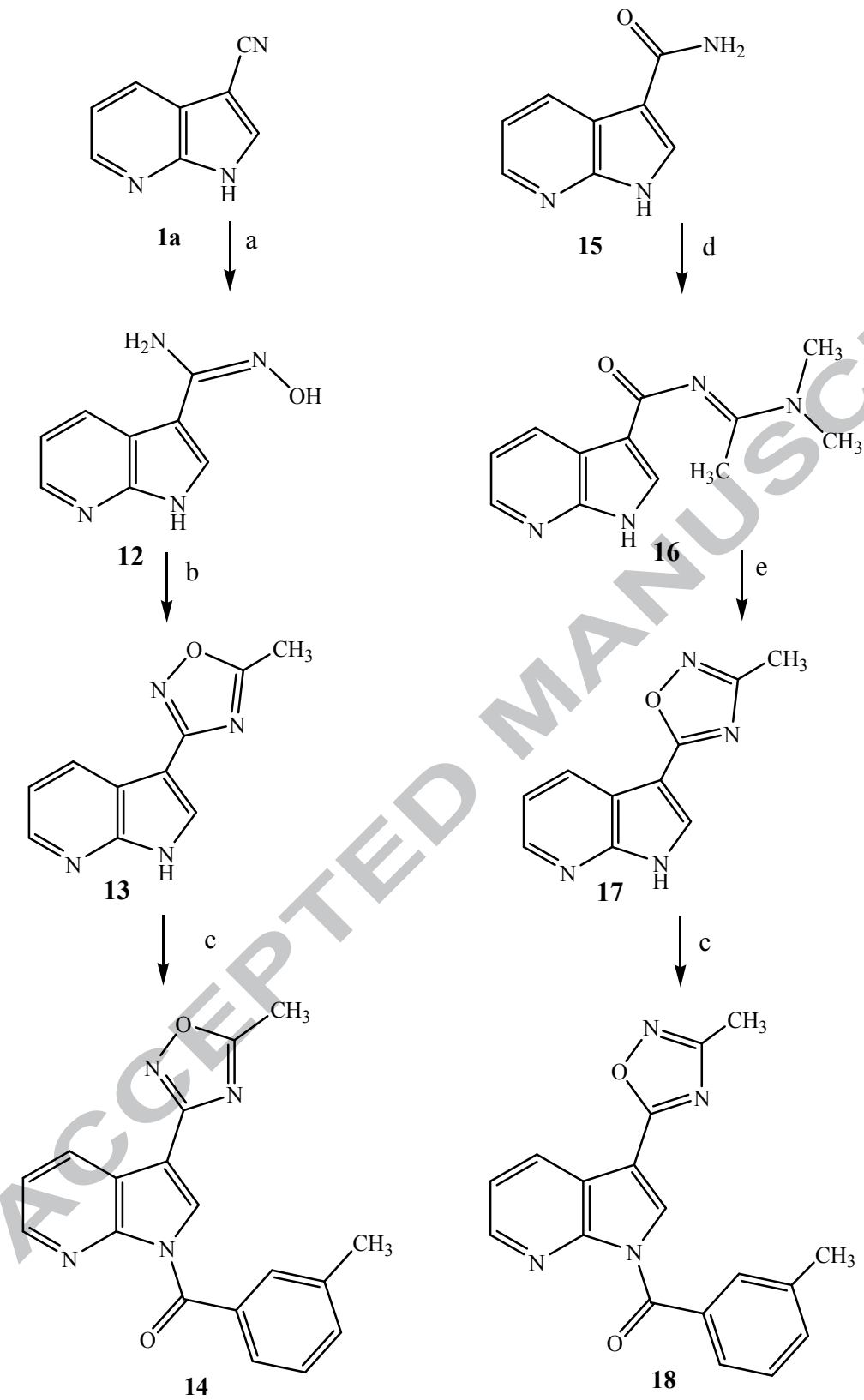

[a]**Reactions and conditions: a)** $NH_2OH.HCl$, EtOH, 0 °C, then Na_2CO_3 in H_2O, reflux, 8 h; **b)** CH_3COOH glacial, dry DMF, DCC, 0 °C, 2 h, then reflux, 6 h; **c)** m-toluoyl chloride, anhydrous CH_2Cl_2, Et_3N, 0 °C, 2 h, then r.t., 2 h; **d)** *N,N*-dimethylacetamide dimethyl acetal, anhydrous toluene, dry DMF, reflux, 2 h; **e)** $NH_2OH.HCl$, dioxane, CH_3COOH, NaOH 10%, reflux, 5 h.

Finally, the introduction at position 3 of other heterocycles, such as pyridine, furan, and thiophene, or 3-CN-phenyl is described in **Scheme 4**. Starting from the precursor **19**[30], a coupling reaction was carried out using the appropriate and commercially available boronic

acid, tetrakis(triphenylphosphine)palladium(0), and 2M Na_2CO_3 in toluene at high temperature (compounds **20a-e**). The deprotection of N1 (**21a-e**[22,31]), followed by benzoylation with m-toluoyl chloride resulted in the compounds **22a-e**.

SCHEME 4[a]

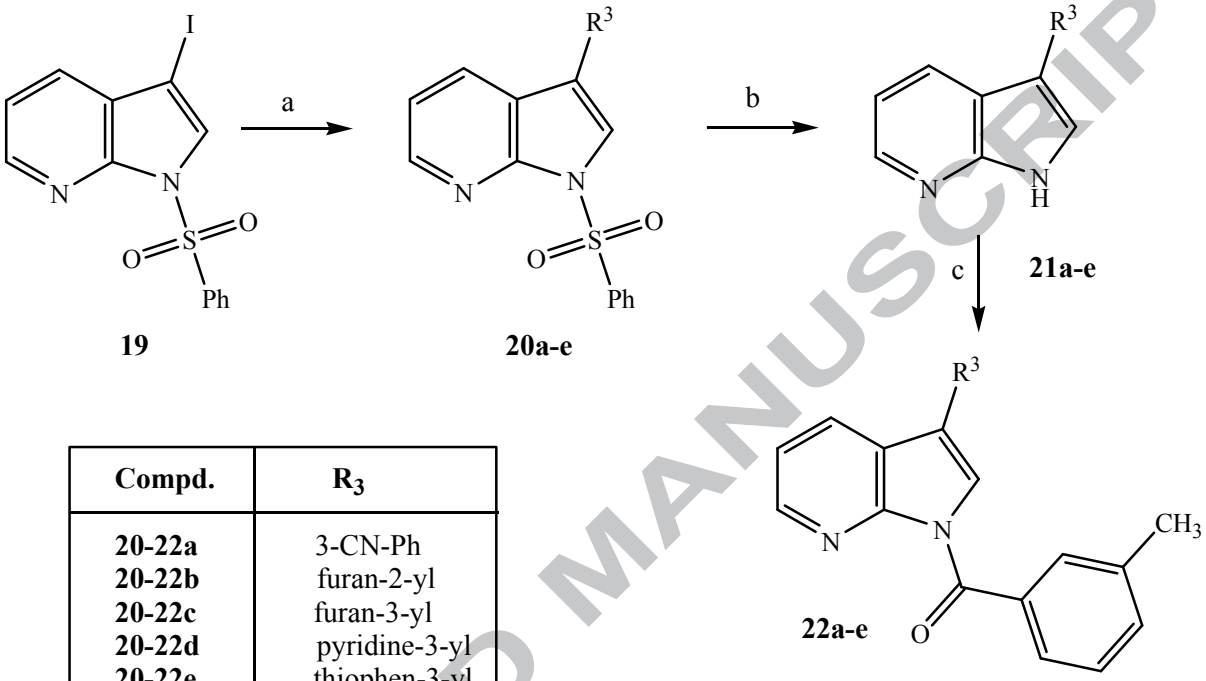

Compd.	R_3
20-22a	3-CN-Ph
20-22b	furan-2-yl
20-22c	furan-3-yl
20-22d	pyridine-3-yl
20-22e	thiophen-3-yl

[a]**Reactions and conditions: a)** R_3-$B(OH)_2$, anhydrous toluene, tetrakis(triphenylphosphine)palladium(0), Na_2CO_3 2M, small amount of EtOH, reflux, 4 h; **b)** TBAF, anhydrous THF, reflux, 2 h; **c)** m-toluoyl chloride, anhydrous CH_2Cl_2, Et_3N, 0 °C, 2 h, then r.t., 2 h.

2.2. Biological activity

All new products were evaluated for HNE inhibitory activity, which was compared with that of Sivelestat, BAY-678 and **FM6**, a potent indazole derivative that we reported previously[15] (**Tables 1** and **2**). The results indicated that the pyrrolo[2,3-b]pyridine nucleus may be an appropriate scaffold for the synthesis of HNE inhibitors, as the majority of new compounds had reasonable inhibitory activity with IC_{50} values in the micromolar/submicromolar range and some compounds active at low nanomolar levels. As an example, a representative concentration–response curve for the inhibition of HNE by compound **2b** is shown in **Figure 3**.

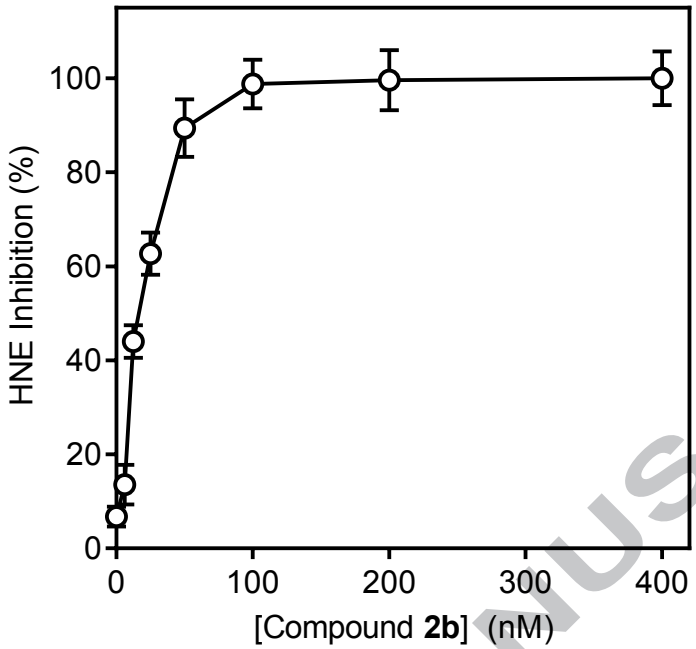

Figure 3. Inhibition of HNE activity by a representative active 1*H*-pyrrolo[2,3-*b*]pyridine (compound **2b**). HNE was incubated with the indicated concentrations of **2b**, and cleavage of the fluorogenic HNE substrate (25 μM) was monitored. The data are presented as the mean ± S.D. of triplicate samples from a representative experiment of three independent experiments.

Analysis of the 3-CN derivatives (**Table 1**) indicated **2a** and **2b**, which are both isomers of **FM6**, were also very potent HNE inhibitors with IC_{50} = 15 and 14 nM, respectively. These results indicate that shifting the nitrogen from position 2 to position 7 did not affect HNE inhibitory activity. In contrast, replacement of the methyl group on the benzoyl fragment with other groups, such as cyano (**2c** and **2d**) or trifluoromethyl (**2e** and **2f**) groups present on other potent HNE inhibitors (**Figure 1**), was not favorable for HNE inhibitory activity in either the *meta* or *para* position. Finally, insertion of alkylcarbonyl groups at position 1 (compounds **2g-l**) was beneficial for activity only in the case of the cyclopropancarbonyl group (compound **2g**, IC_{50} = 87 nM).

Table 1: HNE inhibitory activity of 7-azaindole derivatives **2-4**

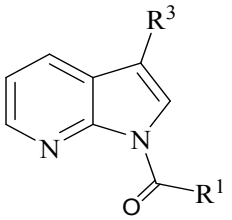

2a-l, 3a-e, 4a,b

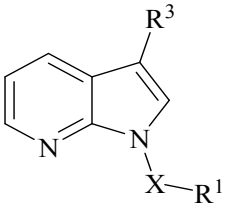

2m, 3f, 4c

Compd.	R^3	R^1	X	IC_{50} (μM)[a]
2a	CN	m-CH_3-Ph	-	0.015±0.004
2b	CN	p-CH_3-Ph	-	0.014±0.004
2c	CN	m-CN-Ph	-	19.1±2.3
2d	CN	p-CN-Ph	-	12.6±2.5
2e	CN	m-CF_3-Ph	-	1.8±0.24
2f	CN	p-CF_3-Ph	-	1.5±0.23
2g	CN	cC_3H_5	-	0.087±0.021
2h	CN	cC_5H_9	-	2.6±0.21
2i	CN	cC_6H_{11}	-	1.5±0.32
2j	CN	CH_3	-	2.4±0.48
2k	CN	nC_3H_7	-	3.4±0.90
2l	CN	nC_4H_9	-	0.49±0.16
2m	CN	Ph	CH_2CONH	N.A.[b]
3a	COOEt	m-CH_3-Ph	-	0.77±0.15
3b	COOEt	p-CH_3-Ph	-	0.64±0.12
3c	COOEt	m-CN-Ph	-	11.5±2.1
3d	COOEt	p-CN-Ph	-	38.5±4.8
3e	COOEt	cC_3H_5	-	0.62±0.14
3f	COOEt	Ph	CH_2CONH	N.A.[b]
4a	CONHPh	m-CH_3-Ph	-	0.39±0.12
4b	CONHPh	cC_3H_5	-	0.80±0.18
4c	CONHPh	-	CH_3	N.A.
Sivelestat				0.050±0.020
BAY-678				0.015±0.002
FM6				0.007±0.001

[a]IC_{50} values are presented as the mean ± SD of three independent experiments. [b]N.A.: no inhibitory activity was found at the highest concentration of compound tested (50 μM).

Analysis of the 3-carbethoxy and 3-carbethoxy phenylamide derivatives (**3a-e**) and (**4a,b**) showed that although good compounds **3a,b,e** and **4a,b** maintained levels of inhibition (IC_{50} = 390-800 nM), they were at least 10 fold less potent than the corresponding 3-CN derivatives. Introduction of the CN group on the benzoyl fragment, as in compounds **3c** and **3d**, was also not favorable for activity. Elimination of the N-CO function at N1 and the introduction at the same position of the CH_2CONH as spacer (compounds **2m** and **3f**, respectively) or a methyl (compound **4c**) led to inactive compounds, confirming that the 1-N-CO moiety was also involved in catalysis for this series of compounds, which is analogous to the potent *N*-benzoylindazoles previously reported.

The data presented above indicate that the methylbenzoyl group was the best substituent for position 1, either when the methyl was in the *meta* or in *para* position. Considering this result and taking into account our previous results for the indazole series, we selected the *m*-methylbenzoyl fragment and, keeping this group at position N1, we further modified position

3 of the 7-azaindole nucleus by inserting a variety of substituents with different characteristics. The data reported in **Table 2** clearly suggest that these modifications were not advantageous for HNE inhibitory activity, as the majority of products were only active in the micromolar range or were inactive (compounds **5a** and **22e**). Only compounds **5e** and **18** were potent HNE inhibitors (IC_{50} = 24 and 80 nM, respectively). The potent activity of **5e** suggests the importance of an electron-withdrawing group at position 3 for HNE inhibitory activity. On the other hand, the difference in activity observed for isomers **14** and **18**, which have the same oxadiazole ring at position 3 although connected differently, is intriguing. In fact, compound **15** is about 45 fold less potent than compound **18**, suggesting a worse orientation and/or interaction at the level of the active site. This aspect is probably related to the free rotation of the oxadiazole ring, isoster of the carbethoxy group, around the simple bond.

Table 2: HNE inhibitory activity of 7-azaindole derivatives **5a-e, 10a, 11, 14, 18, 22a-e**

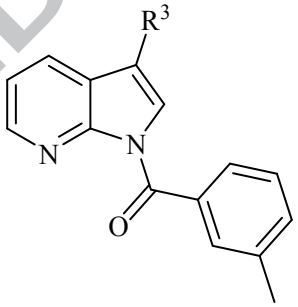

5a-e, 10a, 11, 14, 18, 22a-e

Compd.	R^3	IC_{50} (μM)[a]
5a	H	N.A.
5b	Cl	28.5±1.2
5c	Br	11.9±3.2
5d	I	7.3±2.6
5e	NO_2	0.024±0.009
10a	CH_2-N(CH_3)-Ph	2.4±0.46
11	CH_2-NH-Ph	1.8±0.2
14	5-methyl-1,2,4-oxadiazol-3-yl-	3.6±1.1
18	3-methyl-1,2,4-oxadiazol-5-yl	0.080±0.020
22a	3-CN-Ph	6.7±2.1
22b	furan-2-yl	44.8±3.8
22c	furan-3-yl	42.6±2.8
22d	pyridine-3-yl	6.0±0.7
22e	thiophen-3-yl	N.A.[b]
Sivelestat		0.050±0.020
BAY-678		0.015±0.002

FM6		0.007±0.001

[a]IC_{50} values are presented as the mean ± SD of three independent experiments. [b]N.A.: no inhibitory activity was found at the highest concentration of compound tested (50 µM).

The most potent compounds with $IC_{50} < 0.8$ µM were further evaluated for chemical stability in aqueous buffer using spectrophotometry to detect compound hydrolysis. As shown in **Table 3**, the new pyrrolopyridines were more stable than our previously described HNE inhibitors with the N-benzoylindazole[14,15] and *N*-benzoylpyrazole[32].

Table 3. Half-life ($t_{1/2}$) for the spontaneous hydrolysis of selected derivatives

Compd.	$t_{1/2}$ (h)	Absorbance (nm)[a]
2a	1.9	260
2b	2.6	265
2g	6.8	245
2l	1.9	260
3a	3.5	265
3b	4.3	265
3e	14.4	250
4a	3.4	260
5e	0.4	245
18	2.4	250

[a] Absorption used for monitoring spontaneous hydrolysis.

Ten of the most potent 1*H*-pyrrolo[2,3-*b*]pyridines were also selected for evaluation of reversibility of HNE inhibition over time. Inhibition was maximal for up to 2 h with **2a**, **2l**, **2g**, **5e**, **18**, and >6 h for compound **2b** and reference elastase inhibitors BAY-678 and Sivelestat (**Figure 4**). These results suggest that the active pyrrolo[2,3-*b*]pyridines may be pseudoirreversible inhibitors of HNE [14].

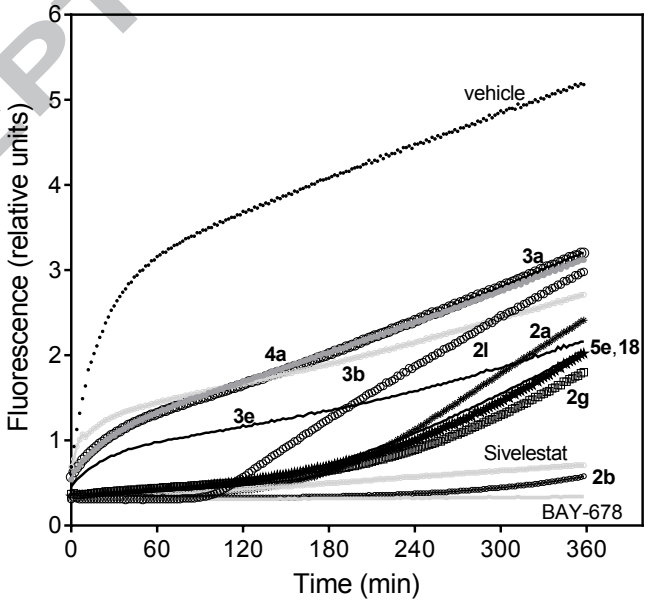

Figure 4. Evaluation of HNE inhibition over time by representative 1*H*-pyrrolo[2,3-*b*]pyridines and reference HNE inhibitors, Sivelestat and BAY-678. HNE was incubated with the indicated compounds (5 µM), and kinetic curves monitoring substrate cleavage catalysed by HNE over time are shown. Representative curves are from two independent experiments.

To further evaluate the mechanism of action of these HNE inhibitors, we performed kinetic experiments. As shown in **Figure 5**, the representative double-reciprocal Lineweaver–

Burk plot of fluorogenic substrate hydrolysis by HNE in the presence of different concentrations of **2b** and **5e** indicates that these compounds are competitive HNE inhibitors. The inhibition constant (K_i) values, determined using Dixon plots for the compounds **2b** and **5e** were ~16 and 51 nM, respectively.

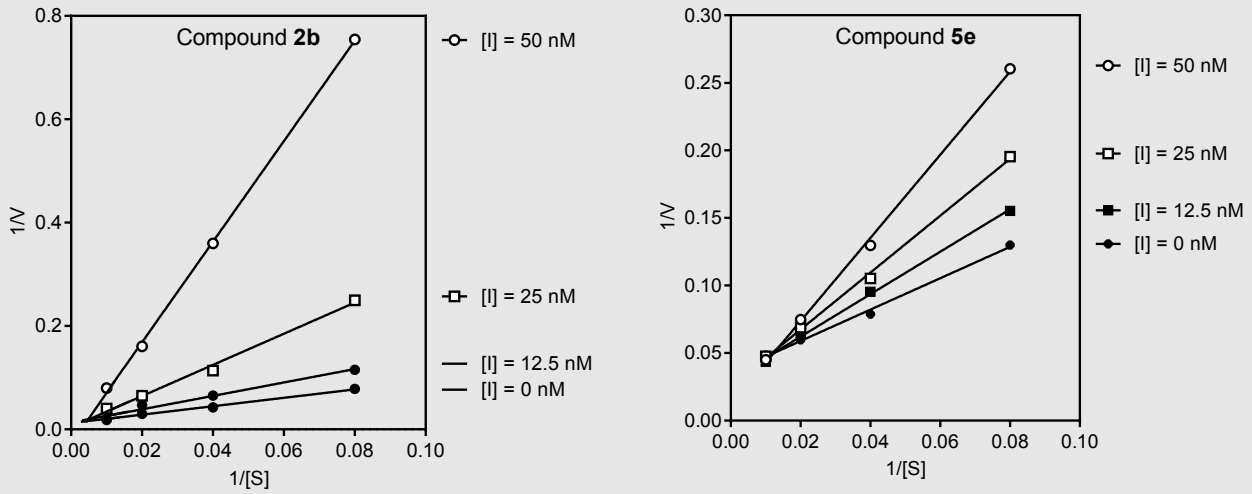

Figure 5. Kinetics of HNE inhibition by compounds **2b** and **5e**. Representative double reciprocal Lineweaver–Burk plots are shown from three independent experiments.

2.3. **Molecular modeling**

The docking strategy was chosen on the basis that the investigated compounds are competitive HNE inhibitors and bind to the same enzyme area as native ligands. Previously, we compared biological data and molecular docking results for compounds **FM6**[15] and **CF7**[16] (see **Figure 6**), which belong to the **A** and **B** series (see **Figure 2**), respectively.

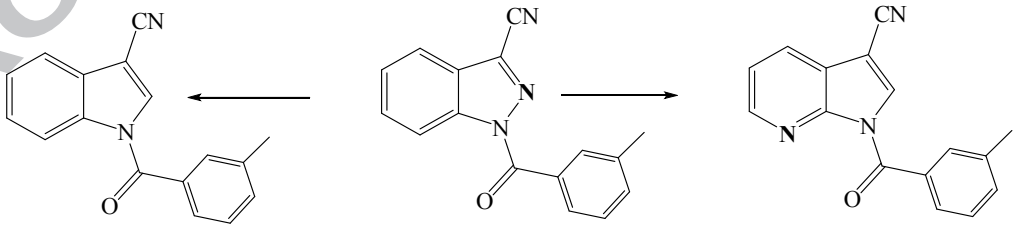

Figure 6. Structures of **CF7**, **FM6**, and **2a**

The difference in activities in this case can be explained by the large length L of the proton transfer channel for the inactive compound **CF7** (**Table 4**). The **FM6** molecule forms an H-bond by its pyrazole-type nitrogen atom in the five-membered ring with Gly193. It also

appears that **CF7** and **FM6**, which differ by the presence or absence of this atom, are differently oriented within the elastase binding site (**Figure 7A**).

These differences are also visible is **Supplementary Figure S1**, which shows key residues of the HNE binding site pockets in the vicinity of the molecular moieties. In **2a**, an additional nitrogen atom is present in the six-membered pyridine moiety. In the docking pose, this atom forms an H-bond with Asp194. Additional H-bonding occurs with Val216 due to the nitrogen atom of the cyano group in **2a** (**Figure 7B**). The length L of the proton transfer channel for **2a** is somewhat larger, and the distance d_1 is smaller than for the active compound **FM6**. In general, the geometry of the inhibitor-enzyme complex is favorable for the formation of a Michaelis complex when the oxygen atom of Ser195 attacks the carbonyl carbon atom of **2a**[32,33]. Despite the difference in the positions of **2a** and **FM6** within the elastase binding site (**Supplementary Figure S1**), the hydroxyl oxygen atom of Ser195 is in a favorable position with respect to the attack for both ligands (**Figure 7B**).

Table 4. Geometric parameters of the enzyme–inhibitor complexes predicted by molecular docking[a]

Compd.	IC_{50} (nM)	d_1 (Å)	α (°)	d_3 (Å)	d_2 (Å)	**L** (Å)[b]
CF7	NA	3.936	78.5	2.480	5.756, 5.919	8.236
FM6	7	3.448	105.2	3.142	2.181, 3.755	5.323
2a	15	2.601	117.0	3.302	3.218, 4.390	6.520
14	3600	3.342	84.4	2.871	2.804, 4.001	5.675
18	80	3.313	71.7	2.968	2.891, 4.023	5.859

[a] The geometric parameters important for formation of a Michaelis complex in the HNE active site were as we reported previously[14], based on the model of synchronous proton transfer from the oxyanion hole in HNE[33]. According to the docking results, a Michaelis complex with Ser195 is formed with participation of the ester carbonyl group. [b]Length of the channel for proton transfer calculated as d_3+min(d_2).

Close analogues **14** and **18** have quite similar docking poses, but the molecules are still displaced relative to each other, because of differences in the electronic structure of the five-membered ring substituents. The key geometric characteristics of the catalytic triad Ser195-His57-Asp102 and the arrangement of ligands relative to Ser195 are also very similar for **14** and **18** (**Table 4**) and should favor activity, except for the fact that the angle α for **18** slightly

A

deviates from the optimum range of 80-120° [33,34]. Nevertheless, compound **14** has a much smaller biological effect than its close analog **18**. This can be explained by a strong anchoring of **14** due to H-bonding with several residues, in particular with Ser195. As a result, the formation of a Michaelis complex from the docking pose by an attack of Ser195 to the carbonyl carbon atom becomes more difficult because mutual reorientation of the inhibitor and binding site should lead to breaking of several H-bonds. **Figure 8** shows a superposition of all three newly investigated compounds (**2a**, **14**, and **18**). Note that the orientation of **2a** (red) resembles the positions of inhibitors **14** and **18**; however, the substituent in the heterocycle (cyano group) is stretched in the opposite direction with respect to the oxadiazole rings of the other two compounds. Perhaps this is due to a formation of the above-mentioned H-bond with the cyano group. In addition, the orientation of the oxadiazole rings in this direction would be hampered sterically due to a clash with Phe215.

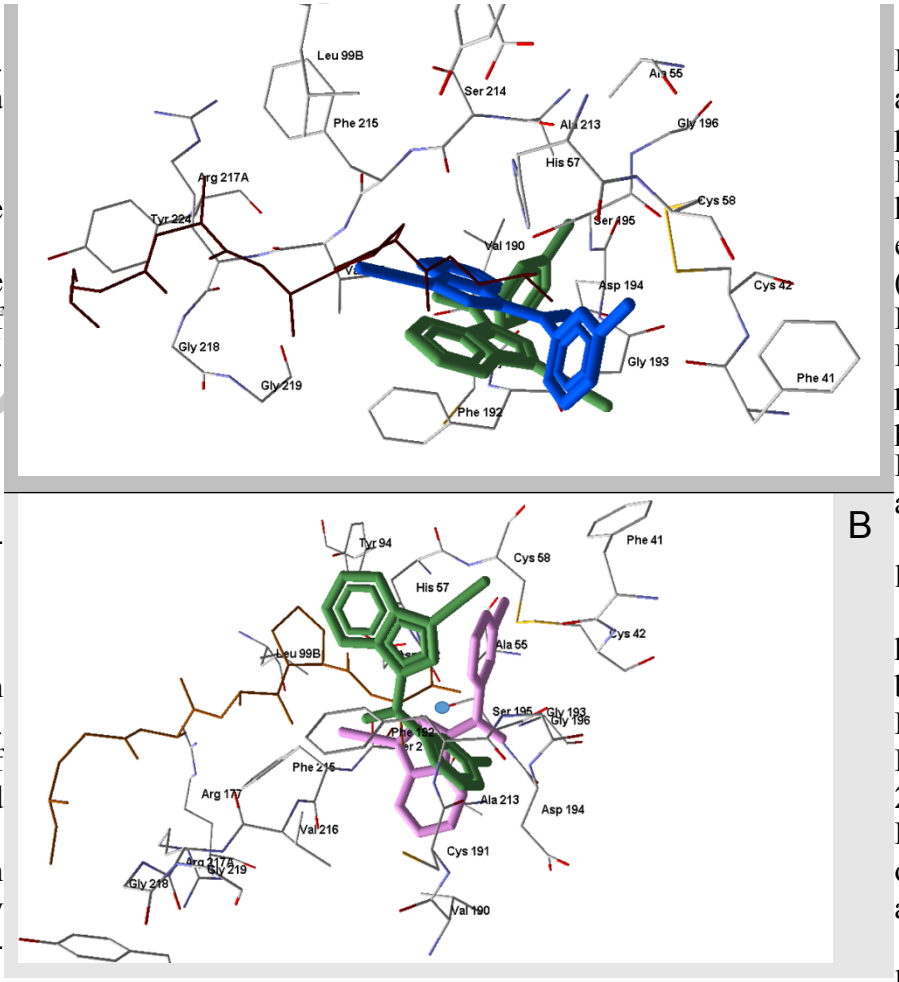

Figure 7. Docking poses of **2a** and published compounds **FM6** and **CF7** in the human neutrophil elastase (1HNE Protein binding site entry of Data Bank[35]). **Panel A**. Docking poses of published **FM6** and **CF7** ligand previously compounds (dark-green) and (blue). Co-crystallized ligand is shown in brown. **Panel B**. Docking peptide ketone is chloromethyl poses of **FM6** shown in (green) and **2a** (magenta). Hydroxyl oxygen atom of Ser195 is marked by a blue circle. Co-crystallized ligand is shown in brown. Residues within 5 Å from the co-crystallized ligand are visible for both panels.

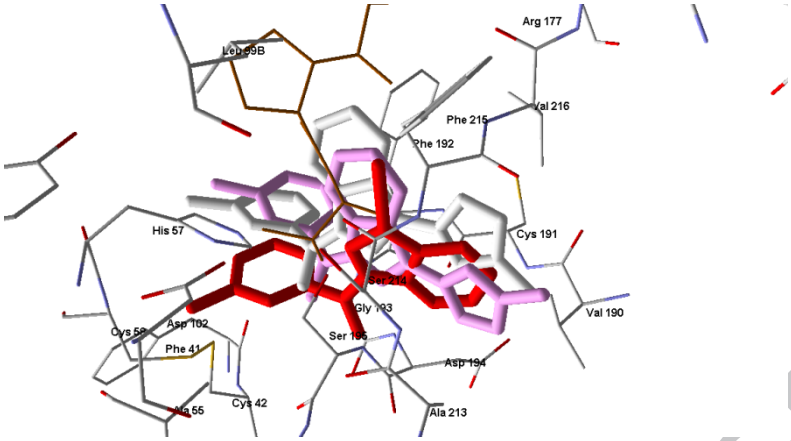

Figure 8. Superposition of docking poses for compounds **2a** (red), **14** (magenta) and **18** (grey) in the human neutrophil elastase binding site (1HNE entry of Protein Data Bank[35]). Co-crystallized ligand peptide chloromethyl ketone is shown in brown. Residues within 5 Å from this ligand are visible.

3. Conclusion

In the present manuscript, we report the pyrrolo[2,3-*b*]pyridine nucleus as a new scaffold for the synthesis of HNE inhibitors. We designed these compounds as isomers of our previously reported indazole-based HNE inhibitors[14,15] in order to assess how a shift of the nitrogen from position 2 to position 7 influences activity. The biological results indicate that these structural modifications do not impact activity since most of the new compounds have IC_{50} values in the micromolar/submicromolar range. The most potent compounds are **2a** and **2b**, which are both isomers of reference compound **FM6**[15], have IC_{50} values of 15 and 14 nM, respectively. The 3-carbethoxy (**3a-e**) and 3-phenylamide derivatives (**4a,b**) also retained good levels of HNE inhibition (IC_{50} = 390-800 nM) but were at least 10 fold less potent than the corresponding 3-CN derivatives. Other modifications at position 3 generally led to low activity or were inactive, and elimination of the N-CO function at N1 position led to completely inactive compounds, confirming that the 1-N-CO moiety was also involved in catalysis for this series of derivatives. Finally, our molecular docking studies showed that the effectiveness of ligand interaction with the HNE binding site depends on H-bonding via the heteroatoms and on orientation of the ligand with respect to the catalytic triad Ser195-His57-Asp102. Despite similarity in positioning of ligands **2a**, **14**, and **18** within the HNE binding site, the docking results indicate that they form H-bonds with different residues of the enzyme, which can contribute to differences in the magnitude of their biological activity.

4. Experimental

4.1. Chemistry

All melting points were determined on a Büchi apparatus (New Castle, DE) and are uncorrected. Extracts were dried over Na_2SO_4, and the solvents were removed under reduced pressure. Merck F-254 commercial plates (Merck, Durham, NC) were used for analytical TLC to follow the course of reactions. Silica gel 60 (Merck 70–230 mesh, Merck, Durham, NC) was used for column chromatography. ^{1}H NMR and ^{13}C NMR spectra were recorded on an Avance 400 instrument (Bruker Biospin Version 002 with SGU, Bruker Inc., Billerica, MA). Chemical shifts (δ) are reported in ppm to the nearest 0.01 ppm using the solvent as an internal standard. Coupling constants (J values) are given in Hz and were calculated using TopSpin 1.3 software (Nicolet Instrument Corp., Madison, WI) and are rounded to the nearest 0.1 vHz. Mass spectra (m/z) were recorded on an ESI-TOF mass spectrometer (Brucker Micro TOF, Bruker Inc., Billerica, MA), and reported mass values are within the error limits of ±5 ppm mass units. Microanalyses indicated by the symbols of the elements or functions were performed with a Perkin–Elmer 260 elemental analyzer (PerkinElmer, Inc., Waltham, MA) for C, H, and N, and the results were within ±0.4% of the theoretical values, unless otherwise stated. Reagents and starting material were commercially available.

4.1.1. General procedure for compounds (2a-l, 3a-e, 4a,b, 5a-e)

To a cooled (0 °C) suspension of **1a-h**[20-26] (0.56 mmol) in anhydrous CH_2Cl_2 (2 mL), 0.72 mmol Et_3N and 1.67 mmol of the appropriate chloride were added. The mixture was stirred at 0 °C for 2 h and then at room temperature for an additional 2 h. The solvent was evaporated, cold water was added, and the mixture was neutralized with 0.5 N NaOH. The reaction mixture was extracted with CH_2Cl_2 (3 x 15 mL), the solvent was dried over sodium sulfate, evaporated *in vacuo*, and the final compounds were purified by crystallization from ethanol (**2a-i**, **3a**,**b**,**e**, and **4b**) or by column chromatography using cyclohexane/ethyl acetate in different ratios: 1:1 (**3d**), 2:1 (**3c** and **4a**), 3:1 (**2l**, **4b**, **5a** and **5e**), 5:1 (**5c**), or 6:1 (**5b** and **5d**) as eluents.

4.1.1.1. 1-(3-Methylbenzoyl)-1*H*-pyrrolo[2,3-*b*]pyridine-3-carbonitrile (2a). Yield = 48%; mp = 127-129 °C (EtOH). ^{1}H NMR (DMSO-d_6) δ 2.36 (s, 3H, CH_3), 7.40-7.46 (m, 2H, Ar), 7.53-7.58 (m, 2H, Ar), 7.63 (s, 1H, Ar), 8.24 (d, 1H, Ar, *J* = 8.0 Hz), 8.36 (d, 1H, Ar, *J* = 4.8 Hz), 8.82 (s, 1H, Ar). ^{13}C NMR (DMSO-d_6) δ 21.21 (CH_3), 101.00 (C), 114.37 (C), 116.00 (CH), 120.89 (CH), 128.31 (CH), 128.86 (CH), 129.03 (CH), 131.19 (CH), 132.76 (C), 135.04 (CH), 138.53 (C), 146.55 (CH), 147.08 (C), 149.00 (C), 167.10 (C). IR = 1693 cm^{-1} (C=O), 2229 cm^{-1} (CN). ESI-MS calcd. for $C_{16}H_{11}N_3O$, 261.28; found: *m/z* 262.09 [M + H]$^{+}$. Anal. $C_{16}H_{11}N_3O$ (C, H, N).

4.1.1.2. 1-(4-Methylbenzoyl)-1*H*-pyrrolo[2,3-*b*]pyridine-3-carbonitrile (2b). Yield = 55%; mp = 146-149 °C (EtOH). ^{1}H NMR (DMSO-d_6) δ 2.41 (s, 3H, CH_3), 7.35 (d, 2H, Ar, *J* = 8.0 Hz), 7.41-7.46 (m, 1H, Ar), 7.70 (d, 2H, Ar, *J* = 8.0 Hz), 8.23 (dd, 1H, Ar, *J* = 1.4 Hz and *J* = 7.8 Hz), 8.31-8.36 (m, 1H, Ar), 8.84 (s, 1H, Ar). ^{13}C NMR (DMSO-d_6) δ 21.80 (CH_3), 101.00 (C), 115.05 (C), 115.62 (CH), 121.21 (C), 123.85 (CH), 128.33 (CH), 129.52 (CH), 129.59 (CH), 129.81 (CH), 129.86 (CH), 130.00 (C), 142.40 (CH), 144.25 (C), 146.66 (C), 167.70 (C). IR = 1697 cm^{-1} (C=O), 2267 cm^{-1} (CN). ESI-MS calcd. for $C_{16}H_{11}N_3O$, 261.28; found: *m/z* 262.09 [M + H]$^{+}$. Anal. $C_{16}H_{11}N_3O$ (C, H, N).

4.1.1.3. 1-(3-Cyanobenzoyl)-1*H*-pyrrolo[2,3-*b*]pyridine-3-carbonitrile (2c). Yield = 10%; oil. ^{1}H NMR ($CDCl_3$-d_1) δ 7.35-7.40 (m, 1H, Ar), 7.66 (t, 1H, Ar, *J* = 7.6 Hz), 7.95 (d, 1H, Ar, *J* = 8.0 Hz), 8.03 (d, 1H, Ar, *J* = 8.0 Hz), 8.12 (s, 1H, Ar), 8.13 (dd, 1H, Ar, *J*= 1.2 Hz and *J* = 8.0 Hz), 8.30 (d, 1H, Ar, *J* = 4.4 Hz), 8.40 (s, 1H, Ar). ^{13}C NMR ($CDCl_3$-d_1) δ 101.02 (C), 113.15 (C), 115.54 (C), 115.68 (CH), 118.61 (C), 121.20 (C), 123.86 (CH), 128.33 (CH), 129.97 (CH), 131.22 (C), 133.10 (CH), 135.43 (CH), 138.05 (CH), 142.46 (CH), 146.66 (C), 167.75 (C). ESI-MS calcd. for $C_{16}H_8N_4O$, 272.26; found: *m/z* 273.07 [M + H]$^{+}$. Anal. $C_{16}H_8N_4O$ (C, H, N).

4.1.1.4. 1-(4-Cyanobenzoyl)-1*H*-pyrrolo[2,3-*b*]pyridine-3-carbonitrile (2d). Yield = 39%; oil. ^{1}H NMR ($CDCl_3$-d_1) δ 7.35-7.40 (m, 1H, Ar), 7.81 (d, 2H, Ar, *J* = 8.0 Hz), 7.89 (d, 2H, Ar, *J* = 8.0 Hz), 8.12 (dd, 1H, Ar, *J* = 1.2 Hz and *J* = 7.6 Hz), 8.29 (d, 1H, Ar, *J* = 4.4

Hz), 8.39 (s, 1H, Ar). ^{13}C NMR ($CDCl_3$-d_1) δ 92.41 (C), 112.95 (C), 116.95 (C), 117.68 (C), 117.75 (C), 120.74 (CH), 121.13 (C), 129.03 (CH), 130.79 (CH), 132.01 (CH), 133.95 (CH), 136.34 (CH), 146.55 (C), 165.36 (C). ESI-MS calcd. for $C_{16}H_8N_4O$, 272.26; found: *m/z* 273.07 $[M + H]^+$. Anal. $C_{16}H_8N_4O$ (C, H, N).

4.1.1.5. 1-(3-(Trifluoromethyl)benzoyl)-1*H*-pyrrolo[2,3-*b*]pyridine-3-carbonitrile (2e). Yield = 45%; mp = 155-157 °C (EtOH). ^{1}H NMR ($CDCl_3$-d_1) δ 7.33-7.38 (m, 1H, Ar), 7.67 (t, 1H, Ar, *J* = 8.0 Hz), 7.94 (d, 1H, Ar, *J* = 8.4 Hz), 8.00 (d, 1H, Ar, *J* = 7.6 Hz), 8.08 (s, 1H, Ar), 8.13 (dd, 1H, Ar, *J* = 1.6 Hz and *J* = 8.0 Hz), 8.33 (dd, 1H, Ar, *J* = 1.6 Hz and *J* = 4.8 Hz), 8.38 (s, 1H, Ar). ^{13}C NMR ($CDCl_3$-d_1) δ 92.54 (C), 113.69 (C), 121.23 (CH), 121.71 (CH), 125.40 (C), 128.33 (C, q, *J* = 31.4 Hz), 128.37 (CH), 130.82 (C, q, *J* = 28.8 Hz), 131.32 (CH), 131.67 (C), 133.67 (CH), 134.32 (CH), 134.86 (CH), 147.09 (CH), 147.19 (C), 166.10 (C). ESI-MS calcd. for $C_{16}H_8F_3N_3O$, 315.25; found: *m/z* 316.07 $[M + H]^+$. Anal. $C_{16}H_8F_3N_3O$ (C, H, N).

4.1.1.6. 1-(4-(Trifluoromethyl)benzoyl)-1*H*-pyrrolo[2,3-*b*]pyridine-3-carbonitrile (2f). Yield = 14%; mp = 120-123 °C (EtOH). ^{1}H NMR ($CDCl_3$-d_1) δ 7.33-7.38 (m, 1H, Ar), 7.78 (d, 2H, Ar, *J* = 8.4 Hz), 7.91 (d, 2H, Ar, *J* = 8.0 Hz), 8.12 (d, 2H, Ar, *J* = 7.6 Hz), 8.35 (s, 1H, Ar). ^{13}C NMR ($CDCl_3$-d_1) δ 101.15 (C), 115.65 (C), 121.23 (C), 121.71 (CH), 125.67 (CH), 124.13 (C, q, *J* = 31.6 Hz), 128.37 (CH), 130.82 (C, q, *J* = 28.8 Hz), 131.32 (CH), 133.67 (CH), 136.32 (C), 142.10 (CH), 146.19 (C), 167.70 (C). ESI-MS calcd. for $C_{16}H_8F_3N_3O$, 315.25; found: *m/z* 316.07 $[M + H]^+$. Anal. $C_{16}H_8F_3N_3O$ (C, H, N).

4.1.1.7. 1-(Cyclopropanecarbonyl)-1*H*-pyrrolo[2,3-*b*]pyridine-3-carbonitrile (2g). Yield = 84%; mp = 142-145 °C (EtOH). ^{1}H NMR (DMSO-d_6) δ 1.23-1.29 (m, 4H, 2 x CH_2), 4.00-4.05 (m, 1H, CH), 7.49-7.54 (m, 1H, Ar), 8.24 (d, 1H, Ar, *J* = 7.6 Hz), 8.55 (d, 1H, Ar, *J* = 4.0 Hz), 8.89 (s, 1H, Ar). ^{13}C NMR (DMSO-d_6) δ 12.60 (CH_2), 15.24 (CH), 89.79 (C), 114.25 (C), 120.94 (CH), 121.67 (C), 129.50 (CH), 135.26 (CH), 146.50 (CH), 146.64 (C), 172.69 (C). IR = 1711 cm^{-1} (C=O), 2226 cm^{-1} (CN). ESI-MS calcd. for $C_{12}H_9N_3O$, 211.22; found: *m/z* 212.08 $[M + H]^+$. Anal. $C_{12}H_9N_3O$ (C, H, N).

4.1.1.8. 1-(Cyclopentanecarbonyl)-1*H*-pyrrolo[2,3-*b*]pyridine-3-carbonitrile (2h). Yield = 39%; mp = 97-100 °C (EtOH). ^{1}H NMR (DMSO-d_6) δ 1.63-1.68 (m, 4H, 2 x CH_2), 1.81-1.86 (m, 2H, CH_2), 1.99-2.04 (m, 2H, CH_2), 4.61-4.66 (m, 1H, CH), 7.46-7.51 (m, 1H, Ar), 8.22 (d, 1H, Ar, *J* = 7.6 Hz), 8.56 (d, 1H, Ar, *J* = 3.6 Hz), 8.92 (s, 1H, Ar). ^{13}C NMR (DMSO-d_6) δ 26.28 (CH_2), 29.98 (CH_2), 45.19 (CH), 89.95 (C), 114.26 (C), 120.80 (CH), 121.61 (C), 129.33 (CH), 135.69 (CH), 146.64 (C), 146.70 (CH), 174.41 (C). IR = 1710 cm^{-1} (C=O), 2230 cm^{-1} (CN). ESI-MS calcd. for $C_{14}H_{13}N_3O$, 239.27; found: *m/z* 240.11 $[M + H]^+$. Anal. $C_{14}H_{13}N_3O$ (C, H, N).

4.1.1.9. 1-(Cyclohexanecarbonyl)-1*H*-pyrrolo[2,3-*b*]pyridine-3-carbonitrile (2i). Yield = 39%; mp = 172-175 °C (EtOH). ^{1}H NMR (DMSO-d_6) δ 1.22-1.28 (m, 1H, CH), 1.34-1.50 (m, 4H, 2 x CH_2), 1.65-1.70 (m, 1H, CH), 1.77-1.82 (m, 2H, CH_2), 1.95-2.00 (m, 2H, CH_2), 4.23-4.28 (m, 1H, CH), 7.48 (dd, 1H, Ar, *J* = 4.8 Hz and *J* = 7.6 Hz), 8.22 (d, 1H, Ar, *J* = 8.0 Hz), 8.57 (d, 1H, Ar, *J* = 4.4 Hz), 8.9 (s, 1H, Ar). ^{13}C NMR (DMSO-d_6) δ 25.49 (CH_2), 25.79 (CH_2), 28.96 (CH_2), 43.95 (CH), 90.05 (C), 114.24 (C), 120.79 (CH), 121.55 (C), 129.34 (CH), 135.53 (CH), 140.00 (C), 146.83 (CH), 174.26 (C). IR = 1711 cm^{-1} (C=O), 2220 cm^{-1} (CN). ESI-MS calcd. for $C_{15}H_{15}N_3O$, 253.30; found: *m/z* 254.12 $[M + H]^+$. Anal. $C_{15}H_{15}N_3O$ (C, H, N).

4.1.1.10. 1-Acetyl-1*H*-pyrrolo[2,3-*b*]pyridine-3-carbonitrile (2j)[26]**.** Yield = 39%; mp = 164-167 °C (EtOH). ^{1}H NMR (DMSO-d_6) δ 2.99 (s, 3H, CH_3), 7.49 (dd, 1H, Ar, *J* = 4.8 Hz and *J* = 8.0 Hz), 8.23 (dd, 1H, Ar, *J* = 1.6 Hz and *J* = 8.0 Hz), 8.56 (dd, 1H, Ar, *J* = 1.6 Hz and *J* = 4.8 Hz), 8.92 (s, 1H, Ar). ^{13}C NMR (DMSO-d_6) δ 26.24 (CH_3), 101.00 (C), 114.23 (C), 120.76 (CH), 121.24 (C), 129.25 (CH), 135.15 (CH), 146.59 (CH), 145.65 (C), 168.55 (C). IR = 1716 cm^{-1} (C=O), 2230 cm^{-1} (CN). ESI-MS calcd. for $C_{10}H_7N_3O$, 185.18; found: *m/z* 186.06 $[M + H]^+$. Anal. $C_{10}H_7N_3O$ (C, H, N).

4.1.1.11. 1-Butyryl-1*H*-pyrrolo[2,3-*b*]pyridine-3-carbonitrile (2k). Yield = 8%; mp = 87-90 °C (EtOH). ^{1}H NMR (DMSO-d_6) δ 0.98 (t, 3H, $COCH_2CH_2CH_3$, *J* = 7.4 Hz), 1.73 (q, 2H, $COCH_2CH_2CH_3$, *J* = 7.4 Hz), 3.49 (t, 2H, $COCH_2CH_2CH_3$, *J* = 7.2 Hz), 7.48 (dd, 1H,

Ar, *J* = 4.8 Hz and *J* = 7.6 Hz), 8.22 (dd, 1H, Ar, *J* = 1.4 Hz e *J* = 7.8 Hz), 8.55 (dd, 1H, Ar, *J* = 1.2 Hz and *J* = 4.8 Hz), 8.93 (s, 1H, Ar). ^{13}C NMR (DMSO-d_6) δ 13.14 (CH_3), 19.40 (CH_2), 34.00 (CH_2), 101.00 (C), 114.23 (C), 120.76 (CH), 121.24 (C), 129.25 (CH), 135.15 (CH), 146.59 (CH), 145.65 (C), 170.35 (C). IR = 1715 cm^{-1} (C=O), 2229 cm^{-1} (CN). ESI-MS calcd. for $C_{12}H_{11}N_3O$, 213.24; found: *m/z* 214.09 $[M + H]^+$. Anal. $C_{12}H_{11}N_3O$ (C, H, N).

4.1.1.12. 1-Pentanoyl-1*H*-pyrrolo[2,3-*b*]pyridine-3-carbonitrile (2l). Yield = 31%; mp = 109-111 °C (EtOH). ^{1}H NMR (DMSO-d_6) δ 0.91 (t, 3H, $COCH_2CH_2CH_2CH_3$, *J* = 7.2 Hz), 1.38-1.43 (m, 2H, $COCH_2CH_2CH_2CH_3$), 1.66-1.71 (m, 2H, $COCH_2CH_2CH_2CH_3$), 3.51 (t, 2H, $COCH_2CH_2CH_2CH_3$, *J* = 7.4 Hz), 7.48 (dd, 1H, Ar, *J* = 4.8 Hz and *J* = 8.0 Hz), 8.22 (d, 1H, Ar, *J* = 6.8 Hz), 8.56 (d, 1H, Ar, *J* = 4.0 Hz), 8.92 (s, 1H, Ar). ^{13}C NMR (DMSO-d_6) δ 13.43 (CH_3), 21.70 (CH_2), 28.25 (CH_2), 31.56 (CH_2), 101.00 (C), 114.23 (C), 120.76 (CH), 121.24 (C), 129.25 (CH), 135.15 (CH), 146.59 (CH), 145.65 (C), 170.45 (C). IR = 1718 cm^{-1} (C=O), 2230 cm^{-1} (CN). ESI-MS calcd. for $C_{13}H_{13}N_3O$, 227.26; found: *m/z* 228.11 $[M + H]^+$. Anal. $C_{13}H_{13}N_3O$ (C, H, N).

4.1.1.13. Ethyl 1-(3-methylbenzoyl)-1*H*-pyrrolo[2,3-*b*]pyridine-3-carboxylate (3a). Yield = 25%; mp = 92-95 °C (EtOH). ^{1}H NMR ($CDCl_3$-d_1) δ 1.42 (t, 3H, OCH_2CH_3, *J* = 7.0 Hz), 2.43 (s, 3H, CH_3), 4.41 (q, 2H, OCH_2CH_3, *J* = 6.8 Hz), 7.31 (t, 1H, Ar, *J* = 6.0 Hz), 7.39 (t, 1H, Ar, *J* = 7.2 Hz), 7.47 (d, 1H, Ar, *J* = 6.8 Hz), 7.56 (d, 1H, Ar, *J* = 7.2 Hz), 7.66 (s, 1H, Ar), 8.30 (s,1H, Ar), 8.41 (s, 1H, Ar), 8.48 (d, 1H, Ar, *J* = 7.6 Hz). ^{13}C NMR ($CDCl_3$-d_1) δ 14.45 (CH_3), 21.37 (CH_3), 60.69 (CH_2), 110.81 (C), 120.13 (CH), 120.74 (C), 127.70 (CH), 128. 31 (CH), 130.60 (CH), 130.90 (CH), 132.80 (C), 133.20 (CH), 134.30 (CH), 138.60 (C), 145.60 (CH), 148.40 (C), 163.70 (C), 167.60 (C). ESI-MS calcd. for $C_{18}H_{16}N_2O_3$, 308.33; found: *m/z* 309.12 $[M + H]^+$. Anal. $C_{18}H_{16}N_2O_3$ (C, H, N).

4.1.1.14. Ethyl 1-(4-methylbenzoyl)-1*H*-pyrrolo[2,3-*b*]pyridine-3-carboxylate (3b). Yield = 30%; mp = 100-103 °C (EtOH). ^{1}H NMR ($CDCl_3$-d_1) δ 1.42 (t, 3H, OCH_2CH_3, *J* = 7.2 Hz), 2.47 (s, 3H, CH_3), 4.41 (q, 2H, OCH_2CH_3, *J* = 7.2 Hz), 7.30-7.35 (m, 3H, Ar), 7.73 (d, 2H, Ar, *J* = 8.4 Hz), 8.32 (s, 1H, Ar), 8,40 (dd, 1H, Ar, *J* = 1.6 Hz and *J* = 4.8 Hz), 8.48

(dd, 1H, Ar, *J* = 1.6 Hz and *J* = 7.6 Hz). ^{13}C NMR ($CDCl_3$-d_1) δ 14.40 (CH_3), 24.30 (CH_3), 60.90 (CH_2), 101.00 (C), 120.13 (CH), 120.74 (C), 126.00 (CH), 128.31 (CH), 130.62 (CH), 130.97 (CH), 132.86 (C), 133.20 (CH), 134.38 (CH), 138.60 (C), 145.60 (CH), 148.49 (C), 162.50 (C), 167.70 (C). ESI-MS calcd. for $C_{18}H_{16}N_2O_3$, 308.33; found: *m/z* 309.12 $[M + H]^+$. Anal. $C_{18}H_{16}N_2O_3$ (C, H, N).

4.1.1.15. Ethyl 1-(3-cyanobenzoyl)-1*H*-pyrrolo[2,3-*b*]pyridine-3-carboxylate (3c). Yield = 15%; oil. ^{1}H NMR ($CDCl_3$-d_1) δ 1.44 (t, 3H, OCH_2CH_3, *J* = 6.8 Hz), 4.44 (q, 2H, OCH_2CH_3, *J* = 7.2 Hz), 7.28-7.33 (m, 1H, Ar), 7.64 (t, 1H, Ar, *J* = 8.0 Hz), 7.93 (d, 1H, Ar, *J* = 7.6 Hz), 8.03 (d, 1H, Ar, *J* = 8.0 Hz), 8.09 (s, 1H, Ar), 8.24 (dd, 1H, Ar, *J* = 1.2 Hz and *J* = 4.4 Hz), 8.48-8.53 (m, 2H, Ar). ^{13}C NMR ($CDCl_3$-d_1) δ14.42 (CH_3), 60.87 (CH_2), 112.37 (C), 112.73 (C), 117.73 (C), 120.48 (CH), 120.88 (C), 129.15 (CH), 130.87 (CH), 132.09 (CH), 134.04 (CH), 134.32 (CH), 134.42 (C), 136.14 (CH), 145.26 (CH), 147.75 (C), 163.29 (C), 165.62 (C). ESI-MS calcd. for $C_{18}H_{13}N_3O_3$, 319.31; found: *m/z* 320.10 $[M + H]^+$. Anal. $C_{18}H_{13}N_3O_3$ (C, H, N).

4.1.1.16. Ethyl 1-(4-cyanobenzoyl)-1*H*-pyrrolo[2,3-*b*]pyridine-3-carboxylate (3d). Yield = 30%; oil. ^{1}H NMR ($CDCl_3$-d_1) δ 1.43 (t, 3H, OCH_2CH_3, *J* = 7.2 Hz), 4.43 (q, 2H, OCH_2CH_3, *J* = 7.2 Hz), 7.27-7.32 (m, 1H, Ar), 7.79 (d, 2H, Ar, *J* = 8.4 Hz), 7.88 (d, 2H, Ar, *J* = 8.0 Hz), 8.23 (d, 1H, Ar, *J* = 4.4 Hz), 8.44-8.49 (m, 2H, Ar). ^{13}C NMR ($CDCl_3$-d_1) δ14.41 (CH_3), 60.87 (CH_2), 112.38 (C), 116.46 (C), 117.87 (C), 120.42 (CH), 120.84 (C), 130.62 (CH), 130.84 (CH), 131.98 (CH), 137.12 (C), 142.28 (CH), 147.82 (C), 163.29 (C), 166.08 (C). ESI-MS calcd. for $C_{18}H_{13}N_3O_3$, 319.31; found: *m/z* 320.10 $[M + H]^+$. Anal. $C_{18}H_{13}N_3O_3$ (C, H, N).

4.1.1.17. Ethyl 1-(cyclopropanecarbonyl)-1*H*-pyrrolo[2,3-*b*]pyridine-3-carboxylate (3e). Yield = 73%; mp = 77-80 °C (EtOH). ^{1}H NMR ($CDCl_3$-d_1) δ 1.23-1.28 (m, 2H, CH_2), 1.39-1.44 (m, 5H, 3H OCH_2CH_3 + 2H CH_2), 4.21-4.26 (m, 1H, CH), 4.40 (q, 2H, OCH_2CH_3, *J* = 7.2 Hz), 7.29-7.34 (m, 1H, Ar), 8.42 (dd, 1H, Ar, *J* = 1.6 Hz and *J* = 4.6 Hz), 8.48 (dd, 1H, Ar, *J* = 1.6 Hz and *J* = 7.6 Hz), 8.63 (s, 1H, Ar). ^{13}C NMR ($CDCl_3$-d_1) δ 12.42 (CH_2),

14.42 (CH_3), 14.94 (CH), 60.61 (CH_2), 110.42 (C), 119.86 (CH), 121.59 (C), 130.69 (CH), 131.20 (CH), 144.64 (CH), 149.00 (C), 164.00 (C), 173.69 (C). IR = 1701 cm^{-1} (C=O amide), 1718 cm^{-1} (C=O ester). ESI-MS calcd. for $C_{14}H_{14}N_2O_3$, 258.27; found: *m/z* 259.10 $[M + H]^+$. Anal. $C_{14}H_{14}N_2O_3$ (C, H, N).

4.1.1.18. 1-(3-Methylbenzoyl)-*N*-phenyl-1*H*-pyrrolo[2,3-*b*]pyridine-3-carboxamide (4a). Yield = 40%; oil. ^1H NMR ($CDCl_3$-d_1) δ 2.41 (s, 1H, CH_3), 7.16 (t, 1H, Ar, *J* = 7.4 Hz), 7.28-7.33 (m, 1H, Ar), 7.35-7.40 (m, 3H, Ar), 7.45 (d, 1H, Ar, *J* = 7.2 Hz), 7.56 (d, 1H, Ar, *J* = 7.6 Hz), 7.64 (d, 3H, Ar, *J* = 7.6 Hz), 7.87 (exch br s, 1H, NH), 8.27 (s, 1H, Ar), 8.34-8.38 (m, 1H, Ar), 8.55 (dd, 1H, Ar, *J* = 1.6 Hz e *J* = 8.0 Hz). ^{13}C NMR ($CDCl_3$-d_1) δ 21.33 (CH_3), 114.77 (C), 120.10 (CH), 120.37 (CH), 121.21 (C), 124.64 (CH), 127.26 (CH), 127.75 (CH), 128.19 (CH), 128.59 (CH), 129.13 (CH), 130.87 (CH), 130.93 (CH), 132.66 (C), 134.39 (CH), 135.65 (CH), 137.67 (C), 138.49 (C), 145.41 (CH), 147.89 (C), 161.52 (C), 167.92 (C). ESI-MS calcd. for $C_{22}H_{17}N_3O_2$, 355.39; found: *m/z* 356.14 $[M + H]^+$. Anal. $C_{22}H_{17}N_3O_2$ (C, H, N).

4.1.1.19. 1-(Cyclopropanecarbonyl)-*N*-phenyl-1*H*-pyrrolo[2,3-*b*]pyridine-3-carboxamide (4b). Yield = 53%; mp = 146-147 °C dec. (EtOH). ^1H NMR ($CDCl_3$-d_1) δ 1.23-1.28 (m, 2H, CH_2), 1.37-1.42 (m, 2H, CH_2), 4.23-4.28 (m, 1H, CH), 7.16 (t, 1H, Ar, *J* = 7.4 Hz), 7.34-7.40 (m, 3H, Ar), 7.64 (d, 2H, Ar, *J* = 7.6 Hz), 7.77 (exch br s, 1H, NH), 8.46 (dd, 1H, Ar, *J* = 1.6 Hz and *J* = 4.8 Hz), 8.55 (s, 1H, Ar), 8.65 (dd, 1H, Ar, *J* = 1.2 Hz and *J* = 8.0 Hz). ^{13}C NMR ($CDCl_3$-d_1) δ 11.42 (CH), 12.61 (CH_2), 115.02 (C), 118.43 (CH), 119.46 (C), 121.59 (CH), 121.62 (CH), 123.80 (CH), 127.34 (CH), 128.00 (CH), 128.93 (CH), 128.97 (CH), 137.99 (C), 142.44 (CH), 146.60 (C), 164.71 (C), 174.69 (C). IR = 1660 cm^{-1} (C=O amide), 1699 cm^{-1} (C=O amide), 3330 cm^{-1} (NH). ESI-MS calcd. for $C_{18}H_{15}N_3O_2$, 305.33; found: *m/z* 306.12 $[M + H]^+$. Anal. $C_{18}H_{15}N_3O_2$ (C, H, N).

4.1.1.20. (1*H*-pyrrolo[2,3-*b*]pyridin-1-yl)(m-tolyl)methanone (5a). Yield = 37%; oil. ^1H NMR ($CDCl_3$-d_1) δ 2.38 (s, 3H, CH_3), 6.57 (d, 1H, Ar, *J* = 4.0 Hz), 7.11-7.17 (m, 1H, Ar), 7.32 (t, 1H, Ar, *J* = 7.8 Hz), 7.38 (d, 1H, Ar, *J* = 7.6 Hz), 7.53 (d, 1H, Ar, *J* = 7.6 Hz), 7.61

(d, 2H, Ar, *J* = 4.0 Hz), 7.87 (dd, 1H, Ar, *J* = 1.8 Hz and *J* = 7.8 Hz), 8.33 (dd, 1H, Ar, *J* = 1.6 Hz and *J* = 4.8 Hz). ^{13}C NMR ($CDCl_3$-d_1) δ 20.92 (CH_3), 99.32 (CH), 115.67 (C), 119.65 (C), 123.84 (CH), 127.26 (CH), 127.75 (CH), 128.19 (CH), 128.59 (CH), 130.87 (CH), 132.66 (C), 134.39 (CH), 142.42 (CH), 146.62 (C), 167.72 (C). ESI-MS calcd. for $C_{15}H_{12}N_2O$, 236.27; found: *m/z* 237.10 $[M + H]^+$. Anal. $C_{15}H_{12}N_2O$ (C, H, N).

4.1.1.21. (3-Chloro-1*H*-pyrrolo[2,3-*b*]pyridin-1-yl)(m-tolyl)methanone (5b). Yield = 25%; oil. ^{1}H NMR ($CDCl_3$-d_1) δ 2.42 (s, 3H, CH_3), 7.24-7.29 (m, 1H, Ar), 7.37 (t, 1H, Ar, *J* = 7.6 Hz), 7.44 (d, 1H, Ar, *J* = 7.2 Hz), 7.55 (d, 1H, Ar, *J* = 7.6 Hz), 7.62 (s, 1H, Ar), 7.69 (s, 1H, Ar), 7.94 (dd, 1H, Ar, *J* = 1.2 Hz and *J* = 6.4 Hz), 8.39 (d, 1H, Ar, *J* = 4.8 Hz). ^{13}C NMR ($CDCl_3$-d_1) δ 20.96 (CH_3), 101.05 (C), 115.68 (CH), 121.24 (C), 123.81 (CH), 128.10 (CH), 128.36 (CH), 129.11 (CH), 130.17 (CH), 130.42 (C), 134.81 (CH), 138.95 (C), 142.46 (CH), 146.63 (C), 167.76 (C). ESI-MS calcd. for $C_{15}H_{11}ClN_2O$, 270.71; found: *m/z* 271.06 $[M + H]^+$. Anal. $C_{15}H_{11}ClN_2O$ (C, H, N).

4.1.1.22. (3-Bromo-1*H*-pyrrolo[2,3-*b*]pyridin-1-yl)(m-tolyl)methanone (5c). Yield = 25%; oil. ^{1}H NMR ($CDCl_3$-d_1) δ 2.42 (s, 3H, CH_3), 7.24-7.29 (m, 1H, Ar), 7.37 (t, 1H, Ar, *J* = 7.6 Hz), 7.44 (d, 1H, Ar, *J* = 7.6 Hz), 7.55 (d, 1H, Ar, *J* = 7.6 Hz), 7.63 (s, 1H, Ar), 7.76 (s, 1H, Ar), 7.89 (dd, 1H, Ar, *J* = 1.6 Hz and *J* = 7.6 Hz), 8.38 (dd, 1H, Ar, *J* = 1.6 Hz and *J* = 4.8 Hz). ^{13}C NMR ($CDCl_3$-d_1) δ 21.77 (CH_3), 96.58 (C), 119.46 (CH), 122.68 (C), 126.78 (CH), 127.46 (CH), 128.05 (CH), 129.11 (CH), 130.59 (CH), 133.42 (C), 133.82 (CH), 138.36 (C), 145.77 (CH), 147.03 (C), 167.08 (C). ESI-MS calcd. for $C_{15}H_{11}BrN_2O$, 315.16; found: *m/z* 317.01 $[M + H]^+$. Anal. $C_{15}H_{11}BrN_2O$ (C, H, N).

4.1.1.23. (3-Iodo-1*H*-pyrrolo[2,3-*b*]pyridin-1-yl)(m-tolyl)methanone (5d). Yield = 47%; oil. ^{1}H NMR ($CDCl_3$-d_1) δ 2.42 (s, 3H, CH_3), 7.26-7.31 (m, 1H, Ar), 7.37 (t, 1H, Ar, *J* = 7.6 Hz), 7.44 (d, 1H, Ar, *J* = 7.2 Hz), 7.55 (d, 1H, Ar, *J* = 7.6 Hz), 7.63 (s, 1H, Ar), 7.76 (dd, 1H, Ar, *J* = 1.6 Hz and *J* = 8.0 Hz), 7.82 (s, 1H, Ar), 8.36 (d, 1H, Ar, *J* = 4.8 Hz). ^{13}C NMR ($CDCl_3$-d_1) δ 21.70 (CH_3), 95.64 (C), 119.46 (CH), 123.68 (C), 126.78 (CH), 127.46 (CH), 128.05 (CH), 129.11 (CH), 131.72 (CH), 133.42 (C), 133.82 (CH), 138.36 (C), 143.70

(CH), 146.31 (C), 167.55 (C). ESI-MS calcd. for $C_{15}H_{11}IN_2O$, 362.17; found: *m/z* 362.99 [M + H]$^+$. Anal. $C_{15}H_{11}IN_2O$ (C, H, N).

4.1.1.24. (3-Nitro-1*H*-pyrrolo[2,3-*b*]pyridin-1-yl)(m-tolyl)methanone (5e). Yield = 35%; mp = 154-155 °C. ^{1}H NMR ($CDCl_3$-d_1) δ 2.44 (s, 3H, CH_3), 7.39-7.46 (m, 2H, Ar), 7.52 (d, 1H, Ar, *J* = 7.6 Hz), 7.59 (d, 1H, Ar, *J* = 8.0 Hz), 7.68 (s, 1H, Ar), 8.47 (dd, 1H, Ar, *J* = 1.6 Hz and *J* = 4.8 Hz), 8.59-8.64 (m, 2H, Ar). ^{13}C NMR ($CDCl_3$-d_1) δ 21.62 (CH_3), 113.61 (C), 115.68 (CH), 126.15 (CH), 128.05 (C), 128.16 (CH), 128.30 (CH), 129.18 (CH), 130.16 (CH), 130.45 (C), 134.89 (CH), 138.91 (C), 142.42 (CH), 148.76 (C), 167.73 (C). ESI-MS calcd. for $C_{15}H_{11}N_3O_3$, 281.27; found: *m/z* 282.08 [M + H]$^+$. Anal. $C_{15}H_{11}N_3O_3$ (C, H, N).

4.1.2. General procedure for compounds (2m, 3f and 4c)

To a suspension of the intermediate **1a-c**[20,21]**,** (0.64 mmol) in anhydrous CH_3CN (3 mL) and 1.28 mmol K_2CO_3, 0.77 mmol 2-chloro-*N*-phenylacetamide (**2m** and **3f**) or methyl iodide (**4c**) were added. The mixture was stirred at reflux for 6-7 h. After evaporation of the solvent, ice-cold water (20 mL) was added, and the precipitate was recovered by vacuum filtration. The final compounds were purified by column chromatography using cyclohexane/ethyl acetate 1:1 (**2m**), cyclohexane/ethyl acetate 1:2 (**3f**), or dichloromethane/methanol 8:2 (**4c**) as eluents.

4.1.2.1. 2-(3-Cyano-1*H*-pyrrolo[2,3-*b*]pyridin-1-yl)-*N*-phenylacetamide (2m). Yield = 58%; mp = 210-213 °C (EtOH). ^{1}H NMR (DMSO-d_6) δ 5.23 (s, 2H, CH_2), 7.04 (t, 1H, Ar, *J* = 7.4 Hz), 7.29 (t, 2H, Ar, *J* = 8.0 Hz), 7.32-7.37 (m, 1H, Ar), 7.54 (d, 2H, Ar, *J* = 8.0 Hz), 8.16 (dd, 1H, Ar, *J* = 1.4 Hz and *J* = 7.8 Hz), 8.41 (dd, 1H, Ar, *J* = 4.8 Hz), 8.49 (s, 1H, Ar), 10.48 (exch br s, 1H, NH). ^{13}C NMR (DMSO-d_6) δ 47.97 (CH_2), 101.10 (C), 115.71 (C), 118.9 (CH), 121.25 (CH), 124.08 (CH), 128.35 (CH), 129.36 (C), 129.75 (CH), 130.43 (CH), 131.00 (CH), 139.02 (C), 139.69 (CH), 145.39 (CH), 149.00 (C), 165.61 (C). IR = 1670 cm^{-1} (C=O), 2216 cm^{-1} (CN), 3290 cm^{-1} (NH). ESI-MS calcd. for $C_{16}H_{12}N_4O$, 276.29; found: *m/z* 277.10 [M + H]$^+$. Anal. $C_{16}H_{12}N_4O$ (C, H, N).

4.1.2.2. Ethyl 1-(2-oxo-2-(phenylamino)ethyl)-1*H*-pyrrolo[2,3-*b*]pyridine-3-carboxylate (3f). Yield = 30%; mp = 205-208 °C (EtOH). ^{1}H NMR (DMSO-d_6) δ 1.33 (t, 3H, OCH_2CH_3, *J* = 7.0 Hz), 4.30 (q, 2H, OCH_2CH_3, *J* = 7.2 Hz), 5.22 (s, 2H, CH_2), 7.04 (t, 1H, Ar, *J* = 7.2 Hz), 7.29 (t, 3H, Ar, *J* = 7.0 Hz), 7.54 (d, 2H, Ar, *J* = 8.0 Hz), 8.32 (d, 3H, Ar, *J* = 8.0 Hz), 10.46 (exch br s, 1H, NH). ^{13}C NMR (DMSO-d_6) δ 14.90 (CH_3), 47.74 (CH_2), 59.93 (CH_2), 105.01 (C), 118.62 (CH), 118.71 (C), 119.50 (CH), 124.00 (CH), 129.36 (CH), 129.62 (CH), 137.56 (CH), 139.11 (C), 144.19 (CH), 148.01 (C), 164.10 (C), 166.00 (C). IR = 1683 cm^{-1} (C=O amide), 1701 cm^{-1} (C=O ester), 3319 cm^{-1} (NH). ESI-MS calcd. for $C_{18}H_{17}N_3O_3$, 323.35; found: *m/z* 324.13 $[M + H]^+$. Anal. $C_{18}H_{17}N_3O_3$ (C, H, N).

4.1.2.3. 1-Methyl-*N*-phenyl-1*H*-pyrrolo[2,3-*b*]pyridine-3-carboxamide(4c). Yield = 43%; mp = 201-204 °C (EtOH). ^{1}H NMR ($CDCl_3$-d_1) δ 4.36 (s, 3H, CH_3), 7.09-7.14 (m, 2H, Ar), 7.35 (t, 2H, Ar, J = 8.0 Hz), 7.65 (d, 2H, Ar, J = 7.6 Hz), 7.70-7.75 (m, 2H, 1H Ar and 1H NH), 8.31 (s, 1H, Ar), 8.90 (d, 1H, Ar, J = 7.2 Hz). ^{13}C NMR ($CDCl_3$-d_1) δ 41.40 (CH_3), 113.45 (CH), 115.91 (C), 119.76 (C), 120.04 (CH), 121.65 (CH), 123.79 (CH), 128.00 (CH), 128.94 (CH), 129.00 (CH), 132.49 (CH), 135.43 (CH), 137.94 (C), 138.49 (C), 164.70 (C). IR = 1683 cm^{-1} (C=O amide), 3321 cm^{-1} (NH). ESI-MS calcd. for $C_{21}H_{19}N_3O$, 329.15; found: m/z 329.96 [M + H]+. Anal. $C_{21}H_{19}N_3O$ (C, H, N).

4.1.3. General procedure for compounds 7a,b

To a solution of the intermediate **6**[27] (0.98 mmol) in anhydrous DCM (5 mL), 3.92 mmol of aniline or *N*-methylaniline and 3.92 mmol of glacial acetic acid were added. The mixture was stirred at room temperature for 30 minutes, then 1.47 mmol of sodium triacetoxyborohydride was added and stirred at room temperature for other 24 h. Cyclohexane (20 mL) was added and the mixture was stirred in this condition for 15-30 minutes. After evaporation of solvent, compounds **7a,b** were purified by column chromatography using toluene/ethyl acetate 9:1 (**7a**) or cyclohexane/ethyl acetate 3:1 (**7b**) as eluents.

4.1.3.1. *N*-methyl-*N*-((1-(phenylsulfonyl)-1*H*-pyrrolo[2,3-*b*]pyridin-3-yl)methyl) aniline (7a). Yield = 65%; oil. ^{1}H NMR ($CDCl_3$-d_1) δ 2.93 (s, 3H, CH_3N), 4.54 (s, 2H, CH_2N), 6.76-6.83 (m, 3H, Ar), 7.10-7.15 (m, 1H, Ar), 7.25 (t, 2H, Ar, *J* = 7.2 Hz), 7.45 (t, 2H, Ar, *J* = 8.0 Hz), 7.51-7.57 (m, 2H, Ar), 7.73 (d, 1H, Ar, *J* = 7.6 Hz), 8.12 (d, 2H, Ar, *J* = 8.0 Hz), 8.41 (dd, 1H, Ar, *J* = 1.2 Hz and *J* = 4.8 Hz). ESI-MS calcd. for $C_{21}H_{19}N_3O_2S$, 377.46; found: *m/z* 378.12 $[M + H]^+$. Anal. $C_{21}H_{19}N_3O_2S$ (C, H, N).

4.1.3.2. *N*-((1-(Phenylsulfonyl)-1*H*-pyrrolo[2,3-*b*]pyridin-3-yl)methyl)aniline (7b) Yield = 70%; oil. ^{1}H NMR ($CDCl_3$-d_1) δ 4.41 (s, 2H, *CH*$_2$NH), 6.67 (d, 2H, Ar, *J* = 8.0 Hz), 6.77 (d, 1H, Ar, *J* = 7.2 Hz), 7.15-7.21 (m, 3H, Ar), 7.45 (t, 2H, Ar, *J* = 8.0 Hz), 7.55 (t, 1H, Ar, *J* = 7.2 Hz), 7.68 (s, 1H, Ar), 7.88 (d, 1H, Ar, *J* = 7.6 Hz), 8.14 (d, 2H, Ar, *J* = 7.6 Hz), 8.43 (d, 1H, Ar, *J* = 4.4 Hz). ESI-MS calcd. for $C_{20}H_{17}N_3O_2S$, 363.43; found: *m/z* 364.11 $[M + H]^+$. Anal. $C_{20}H_{17}Cl_2N_3O_2S$ (C, H, N).

4.1.4. Allyl phenyl((1-(phenylsulfonyl)-1*H*-pyrrolo[2,3-*b*]pyridin-3-yl)methyl)carbamate (8).

To a suspension of 0.30 mmol allyl chloroformate in 0.3 mL dioxane, 0.45 mmol sodium azide in 0.3 mL water was added and stirred at room temperature for 1 h. A solution of **7b** (0.36 mmol) in 0.7 mL Na_2CO_3 1% and 0.7 mL dioxane was then added, and the mixture was stirred at room temperature overnight. After addition of a bit of water, the precipitate was recovered by vacuum filtration and crystallized with ethanol to obtain the desired compound. Yield = 83%; mp = 119-122 °C (EtOH). ^{1}H NMR (DMSO-d_6) δ 4.57 (d, 2H, *CH*$_2$=CH, *J* = 4.8 Hz), 4.99 (s, 2H, *CH*$_2$-N), 5.06-5.11 (m, 2H, O-*CH*$_2$-CH), 5.80-5.88 (m, 1H, CH_2=*CH*), 7.04 (d, 2H, Ar, *J* = 7.6 Hz), 7.20-7.28 (m, 4H, Ar), 7.53-7.59 (m, 3H, Ar), 7.67 (t, 1H, Ar, *J* = 7.2 Hz), 7.86 (d, 3H, Ar, *J* = 7.6 Hz), 8.32 (d, 1H, Ar, *J* = 3.6 Hz). ESI-MS calcd. for $C_{24}H_{21}N_3O_4S$, 447.51; found: *m/z* 448.13 $[M + H]^+$. Anal. $C_{24}H_{21}N_3O_4S$ (C, H, N).

4.1.5. General procedure for compounds 9a,b

To a solution of intermediate **7a** or **8** (0.30 mmol) in anhydrous THF (3 mL), 0.90 mmol TBAF was added, and the mixture was stirred at reflux for 3-4 h. After cooling, the solvent

was evaporated, and cold-ice water was added (20 mL). The product was recovered by extraction with DCM (3 x 15 mL). The solvent was evaporated *in vacuo* to obtain the desired compounds, which were purified by column chromatography using cyclohexane/ethyl acetate 1: 3 as eluent.

4.1.5.1. *N*-((1*H*-pyrrolo[2,3-*b*]pyridin-3-yl)methyl)-*N*-methylaniline (9a). Yield = 44%; oil. ^{1}H NMR ($CDCl_3$-d_1) δ 2.94 (s, 3H, CH_3N-Ph), 4.64 (s, 2H, CH_2N-Ph), 6.76 (t, 1H, Ar, *J* = 7.2 Hz), 6.88 (d, 2H, Ar, *J* = 8.4 Hz), 7.02-7.07 (m, 1H, Ar), 7.19 (s, 1H, Ar), 7.25 (t, 2H, Ar, *J* = 7.6 Hz), 7.86 (d, 1H, Ar, *J* = 8.0 Hz), 8.28 (d, 1H, Ar, *J* = 4.8 Hz), 9.93 (exch br s, 1H, NH). ESI-MS calcd. for $C_{15}H_{15}N_3$, 237.30; found: *m/z* 238.13 $[M + H]^+$. Anal. $C_{15}H_{15}N_3$ (C, H, N).

4.1.5.2. Allyl ((1*H*-pyrrolo[2,3-*b*]pyridin-3-yl)methyl)(phenyl)carbamate (9b). Yield = 44%; oil. ^{1}H NMR ($CDCl_3$-d_1) δ 4.63 (d, 2H, CH_2=CH, *J* = 4.8 Hz), 5.01 (s, 2H, CH_2-N), 5.09-5.14 (m, 2H, O-CH_2-CH), 5.85-5.90 (m, 1H, CH_2=CH), 6.70-6.76 (m, 1H, Ar), 7.01-7.10 (m, 3H, Ar), 7.15 (s, 1H, Ar), 7.18-7.28 (m, 3H, Ar), 8.28-8.33 (m, 1H, Ar), 11.30 (exch br s, 1H, NH). ESI-MS calcd. for $C_{18}H_{17}N_3O_2$, 307.35; found: *m/z* 308.14 $[M + H]^+$. Anal. $C_{18}H_{17}N_3O_2$ (C, H, N).

4.1.6. General procedure for compounds 10a,b

Compounds **10a,b** were obtained starting from **9a** and **9b**, respectively, and using m-toluoyl chloride as a reactant, following the same procedure described for compounds **2a-l, 3a-e, 4a,b, 5a-e**. After dilution and neutralization with NaOH, the suspension was extracted with CH_2Cl_2 (3 x 15 mL), and evaporation of the solvent resulted in final compounds **11a**,**b**, which were purified by column chromatography using toluene/ethyl acetate 9:1 (**11a**) or hexane/acetone 4:1 (**11b**) as eluents.

4.1.6.1. (3-((Methyl(phenyl)amino)methyl)-1*H*-pyrrolo[2,3-*b*]pyridin-1-yl)(m-tolyl) methanone (10a). Yield = 65%; oil. ^{1}H NMR ($CDCl_3$-d_1) δ 2.39 (s, 3H, m-CH_3-Ph), 2.96 (s, 3H, CH_3N-Ph), 4.60 (s, 2H, CH_2N-Ph), 6.79 (t, 1H, Ar, *J* = 6.8 Hz), 6.88 (d, 2H, Ar, *J* = 8.0 Hz), 7.11-7.16 (m, 1H, Ar), 7.23-7.28 (m, 2H, Ar), 7.33 (t, 1H, Ar, *J* = 7.6 Hz), 7.40 (d, 1H,

Ar, *J* = 7.6 Hz), 7.48-7.53 (m, 2H, Ar), 7.59 (s, 1H, Ar), 7.82 (d, 1H, Ar, *J* = 7.6 Hz), 8.34 (dd, 1H, Ar, *J* = 1.2 Hz and *J* = 4.4 Hz). ^{13}C NMR ($CDCl_3$-d_1) δ 21.35 (CH_3), 38.28 (CH_3), 49.14 (CH_2), 113.68 (CH), 118.86 (CH), 122.55 (C), 125.61 (CH), 127.07 (CH), 127.37 (CH), 127.97 (CH), 128.02 (CH), 129.31 (CH), 130.64 (CH), 133.42 (CH), 133.92 (C), 138.12 (C), 144.89 (CH), 149.89 (C), 167.63 (C). ESI-MS calcd. for $C_{23}H_{21}N_3O$, 355.43; found: *m/z* 356.17 $[M + H]^+$. Anal. $C_{23}H_{21}N_3O$ (C, H, N).

4.1.6.2. Allyl ((1-(3-methylbenzoyl)-1*H*-pyrrolo[2,3-*b*]pyridin-3-yl)methyl)(phenyl) carbamate (10b). Yield = 33%; oil. ^{1}H NMR ($CDCl_3$-d_1) δ 2.39 (s, 3H, *CH*$_3$-Ph), 4.62 (d, 2H, *CH*$_2$=CH, *J* = 4.4 Hz), 4.97 (s, 2H, *CH*$_2$-N), 5.10-5.15 (m, 2H, O-*CH*$_2$-CH), 5.79-5.84 (m, 1H, CH_2=*CH*), 7.02 (d, 2H, Ar, *J* = 6.4 Hz), 7.14-7.19 (m, 1H, Ar), 7.25-7.33 (m, 5H, Ar), 7.39 (t, 2H, Ar, *J* = 7.2 Hz), 7.52 (s, 1H, Ar), 7.90 (s, 1H, Ar), 8.39 (dd, 1H, Ar, *J* = 1.2 Hz and *J* = 4.8 Hz). ESI-MS calcd. for $C_{26}H_{23}N_3O_3$, 425.48; found: *m/z* 426.18 $[M + H]^+$. Anal. $C_{26}H_{23}N_3O_3$ (C, H, N).

4.1.7. (3-((Phenylamino)methyl)-1*H*-pyrrolo[2,3-*b*]pyridin-1-yl)(m-tolyl)methanone (11)

A mixture of **10b** (0.05 mmol), phenylsilane (0.5 mmol), and Tetrakis(triphenylphosphine)palladium(0) (0.005 mmol) in CH_2Cl_2 (3 mL) was stirred at room temperature for 1 h. After dilution with ice-cold water, the suspension was extracted with CH_2Cl_2 (3 x 15 mL), dried over sodium sulfate, and the solvent was evaporated *in vacuo* to obtain **11**, which was purified by column chromatography using toluene/ethyl acetate 9:1 as eluent. Yield = 35%; oil. ^{1}H NMR ($CDCl_3$-d_1) δ 2.40 (s, 3H, *CH*$_3$-Ph), 4.47 (s, 2H, CH_2-N), 6.76 (d, 2H, Ar, *J* = 8.0 Hz), 6.81 (t, 1H, Ar, *J* = 7.6 Hz), 7.17-7.23 (m, 2H, Ar), 7.34 (t, 2H, Ar, *J* = 7.6 Hz), 7.41 (d, 1H, Ar, *J* = 7.2 Hz), 7.52 (d, 1H, Ar, *J* = 7.6 Hz), 7.59-7.64 (m, 2H, Ar), 7.97 (d, 1H, Ar, *J* = 7.6 Hz), 8.37 (d, 1H, Ar, *J* = 4.0 Hz). ^{13}C NMR ($CDCl_3$-d_1) δ 21.03 (CH_3), 39.47 (CH_2), 112.65 (C), 113.52 (CH), 113.59 (CH), 115.61 (CH), 120.22 (C), 120.87 (CH), 122.53 (CH), 128.10 (CH), 128.34 (CH), 129.19 (CH), 129.56 (CH), 130.13 (CH), 130.45 (C), 134.82 (CH), 138.90 (C), 142.44 (CH), 147.68 (C), 149.34 (C), 167.72 (C).

ESI-MS calcd. for $C_{22}H_{19}N_3O$, 341.41; found: *m/z* 342.16 $[M + H]^+$. Anal. $C_{22}H_{19}N_3O$ (C, H, N).

4.1.8. 5-Methyl-3-(1*H*-pyrrolo[2,3-*b*]pyridin-3-yl)-1,2,4-oxadiazole (13)

To a cooled (0 °C) solution of acetic acid in DMF (1 mL), 0.58 mmol N,N'-dicyclohexylcarbodiimide (DCC) was added, followed by addition of 0.39 mmol **12**[28] and stirring at 0 °C for another hour, then at room temperature for 2 h and at reflux for 6 h. After cooling, ice-cold water was added, the precipitate was recovered by vacuum filtration, and the final compound was purified by column chromatography using CH_2Cl_2/MeOH 9:1 as eluent. Yield = 51%; mp = 194-197 °C (EtOH). ^{1}H NMR (DMSO-d_6) δ 2.62 (s, 3H, CH_3), 7.21-7.26 (m, 1H, Ar), 8.15 (s, 1H, Ar), 8.30-8.35 (m, 2H, Ar), 12.38 (exch br s, 1H, NH). ESI-MS calcd. for $C_{10}H_8N_4O$, 200.20; found: *m/z* 201.07 $[M + H]^+$. Anal. $C_{10}H_8N_4O$ (C, H, N).

4.1.9. (E)-*N*-(1-(dimethylamino)ethylidene)-1*H*-pyrrolo[2,3-*b*]pyridine-3-carboxamide (16)

To a suspension of 0.68 mmol intermediate **15**[29] in anhydrous toluene (2 mL), 0.3 mL dry DMF (catalytic amount) and 2.38 mmol N,N-dimethylacetamide dimethyl acetal were added. The mixture was stirred at reflux for 2 h. After cooling, ice-cold water (20 mL) was added, and the suspension was extracted with ethyl acetate (3 x 15 mL). Evaporation of the solvent resulted in the desired compound, which was purified by column chromatography using CH_2Cl_2/MeOH 95:5 as eluent. Yield = 38%; oil. ^{1}H NMR ($CDCl_3$-d_1) δ 2.34 (s, 3H, N=C-CH_3), 3.15 (d, 6H, $N(CH_3)_2$), 7.16-7.21 (m, 1H, Ar), 8.10 (s, 1H, Ar), 8.33 (dd, 1H, Ar, *J* = 1.2 Hz and *J* = 4.4 Hz), 8.65 (dd, 1H, Ar, *J* = 1.6 Hz and *J* = 8.0 Hz), 12.04 (exch br s, 1H, NH). ESI-MS calcd. for $C_{12}H_{14}N_4O$, 230.27; found: *m/z* 231.12 $[M + H]^+$. Anal. $C_{12}H_{14}N_4O$ (C, H, N).

4.1.10. 3-Methyl-5-(1*H*-pyrrolo[2,3-*b*]pyridin-3-yl)-1,2,4-oxadiazole (17)

A mixture of 0.26 mmol compound **17**, 0.39 mmol hydroxylamine hydrochloride, 1.2 mL acetic acid, and 0.25 mL NaOH 10% in 1.5 mL dioxane was heated at reflux under stirring

for 5 h. After cooling, ice-cold water (20 mL) was added, and the precipitate was recovered by vacuum filtration to obtain the pure compound. Yield = 57%; mp = 206-209 °C (EtOH). ^{1}H NMR (DMSO-d_6) δ 2.38 (s, 3H, CH_3), 7.27-7.32 (m, 1H, Ar), 8.36-8.41 (m, 2H, Ar), 8.47 (s, 1H, Ar), 12.75 (exch br s, 1H, NH). ESI-MS calcd. for $C_{10}H_8N_4O$, 200.20; found: *m/z* 201.07 $[M + H]^+$. Anal. $C_{10}H_8N_4O$ (C, H, N).

4.1.11. General procedure for compounds 14 and 18

Compound **14** and **18** were obtained starting from **13** and **17**, respectively, using m-toluoyl chloride as the reactant, following the same procedure described for compounds **2a-l, 3a-e, 4a,b, 5a-e**. After dilution and neutralization with NaOH, the suspension was extracted with CH_2Cl_2 (3 x 15 mL), and evaporation of the solvent resulted in final compounds **14** and **18**, which were purified by column chromatography using cyclohexane/ethyl acetate 4:1 as eluent.

4.1.11.1. (3-(5-Methyl-1,2,4-oxadiazol-3-yl)-1*H*-pyrrolo[2,3-*b*]pyridin-1-yl)(m-tolyl) methanone (14). Yield = 47%; mp = 139-142 °C (EtOH). ^{1}H NMR ($CDCl_3$-d_1) δ 2.43 (s, 3H, m-*CH*$_3$-Ph), 2.66 (s, 3H, CH_3), 7.33-7.41 (m, 2H, Ar), 7.46 (d, 1H, Ar, *J* = 7.2 Hz), 7.59 (d, 1H, Ar, *J* = 7.6 Hz), 7.67 (s, 1H, Ar), 8.32 (s, 1H, Ar), 8.47 (d, 1H, Ar, *J* = 4.4 Hz), 8.57 (d, 1H, Ar, *J* = 8.0 Hz). ^{13}C NMR ($CDCl_3$-d_1) δ 12.22 (CH_3), 21.34 (CH_3), 107.01 (C), 119.99 (CH), 120.23 (C), 127.50 (CH), 128.33 (CH), 129.28 (CH), 130.77 (CH), 131.07 (CH), 133.10 (C), 134.09 (CH), 138.56 (C), 145.69 (CH), 148.47 (C), 163.87 (C), 167.51 (C), 176.09 (C). ESI-MS calcd. for $C_{18}H_{14}N_4O_2$, 318.33; found: *m/z* 319.12 $[M + H]^+$. Anal. $C_{18}H_{14}N_4O_2$ (C, H, N).

4.1.11.2. (3-(3-methyl-1,2,4-oxadiazol-5-yl)-1*H*-pyrrolo[2,3-*b*]pyridin-1-yl)(m-tolyl) methanone (18). Yield = 42%; mp = 151-153 °C (EtOH). ^{1}H NMR ($CDCl_3$-d_1) δ 2.44 (s, 3H, m-*CH*$_3$-Ph), 2.49 (s, 3H, CH_3), 7.36-7.42 (m, 2H, Ar), 7.49 (d, 1H, Ar, *J* = 7.6 Hz), 7.60 (d, 1H, Ar, *J* = 7.6 Hz), 7.68 (s, 1H, Ar), 8.44 (s, 1H, Ar), 8.48 (dd, 1H, Ar, *J* = 1.6 Hz and *J* = 4.8 Hz), 8.61 (dd, 1H, Ar, J = 1.6 Hz and *J* = 7.6 Hz). ^{13}C NMR ($CDCl_3$-d_1) δ 11.68 (CH_3), 21.36 (CH_3), 104.38 (C), 119.59 (C), 120.34 (CH), 127.68 (CH), 128.39 (CH), 130.31 (CH),

130.53 (CH), 130.90 (CH), 132.66 (C), 134.48 (CH), 138.67 (C), 146.26 (CH), 148.37 (C), 167.31 (C), 167.57 (C), 171.04 (C). ESI-MS calcd. for $C_{18}H_{14}N_4O_2$, 318.33; found: *m/z* 319.12 $[M + H]^+$. Anal. $C_{18}H_{14}N_4O_2$ (C, H, N).

4.1.12. General procedure for compounds (20a-e)

To a suspension of intermediate **19**[30] (0.34 mmol) in 3 mL toluene, 0.051 mol tetrakis(triphenylphosphine)palladium(0), 3 mL 2M Na_2CO_3 solution, and 0.68 mmol of the appropriate hetero(phenyl)-boronic acid were added. The mixture was stirred at reflux for 4 h. After cooling, ice-cold water (20 mL) was added, the suspension was extracted with CH_2Cl_2 (3 x 15 mL), dried over sodium sulfate, and the solvent was evaporated *in vacuo* to obtain the final compounds, which were purified by column chromatography using cyclohexane/ethyl acetate 3:1 (**20a-d**) or hexane/acetone 4:1 (**20e**) as eluents.

4.1.12.1. 3-(1-(Phenylsulfonyl)-1*H*-pyrrolo[2,3-*b*]pyridin-3-yl)benzonitrile (20a). Yield = 74%; oil. ^{1}H NMR ($CDCl_3$-d_1) δ 7.25-7.30 (m, 1H, Ar), 7.51 (t, 2H, Ar, *J* = 8.0 Hz), 7.56-7.62 (m, 2H, Ar), 7.65 (d, 1H, Ar, *J* = 7.6 Hz), 7.82 (dd, 1H, Ar, *J* = 1.2 Hz and *J* = 6.4 Hz), 7.86 (s, 1H, Ar), 7.94 (s, 1H, Ar), 8.06 (dd, 1H, Ar, *J* = 1.2 Hz and *J* = 8.0 Hz), 8.26 (d, 2H, Ar, *J* = 7.2 Hz), 8.51 (dd, 1H, Ar, *J* = 1.2 Hz and *J* = 4.8 Hz). ESI-MS calcd. for $C_{20}H_{13}N_3O_2S$, 359.40; found: *m/z* 360.08 $[M + H]^+$. Anal. $C_{20}H_{13}N_3O_2S$ (C, H, N).

4.1.12.2. 3-(Furan-2-yl)-1-(phenylsulfonyl)-1*H*-pyrrolo[2,3-*b*]pyridine (20b). Yield = 90%; oil. ^{1}H NMR ($CDCl_3$-d_1) δ 6.48-6.53 (m, 1H, Ar), 6.61 (d, 1H, Ar, *J* = 3.2 Hz), 7.22-7.26 (m, 1H, Ar), 7.43-7.49 (m, 3H, Ar), 7.55 (t, 1H, Ar, *J* = 7.2 Hz), 7.99 (s, 1H, Ar), 8.16-8.21 (m, 3H, Ar), 8.46 (dd, 1H, Ar, *J* = 1.2 Hz and *J* = 4.8 Hz). ESI-MS calcd. for $C_{17}H_{12}N_2O_3S$, 324.35; found: *m/z* 325.06 $[M + H]^+$. Anal. $C_{17}H_{12}N_2O_3S$ (C, H, N).

4.1.12.3. 3-(Furan-3-yl)-1-(phenylsulfonyl)-1*H*-pyrrolo[2,3-*b*]pyridine (20c). Yield = 94%; mp = 137-140 °C (EtOH). ^{1}H NMR ($CDCl_3$-d_1) δ 6.68 (s, 1H, Ar), 7.21-7.26 (m, 1H, Ar), 7.47 (t, 2H, Ar, *J* = 7.6 Hz), 7.52-7.58 (m, 2H, Ar), 7.77 (s, 1H, Ar), 7.82 (s, 1H, Ar), 7.96 (dd, 1H, Ar, *J* = 1.2 Hz and *J* = 8.4 Hz), 8.21 (d, 2H, Ar, *J* = 7.6 Hz), 8.46 (dd, 1H, Ar,

J = 1.2 Hz and *J* = 4.8 Hz). ESI-MS calcd. for $C_{17}H_{12}N_2O_3S$, 324.35; found: *m/z* 325.06 $[M + H]^+$. Anal. $C_{17}H_{12}N_2O_3S$ (C, H, N).

4.1.12.4. 1-(Phenylsulfonyl)-3-(pyridin-3-yl)-1*H*-pyrrolo[2,3-*b*]pyridine (20d). Yield = 88%; oil. ^{1}H NMR ($CDCl_3$-d_1) δ 7.25-7.30 (m, 1H, Ar), 7.40-7.46 (m, 1H, Ar), 7.48-7.59 (m, 2H, Ar), 7.63-7.74 (m, 1H, Ar), 7.90 (dd, 1H, Ar, *J* = 1.6 Hz and *J* = 8.0 Hz), 7.94 (s, 1H, Ar), 8.06 (d, 1H, Ar, *J* = 8.0 Hz), 8.19 (d, 2H, Ar, *J* = 8.4 Hz), 8.50 (d, 1H, Ar, *J* = 4.8 Hz), 8.61 (d, 1H, Ar, *J* = 4.8 Hz), 8.87 (s, 1H, Ar). ESI-MS calcd. for $C_{18}H_{13}N_3O_2S$, 335.38; found: *m/z* 336.08 $[M + H]^+$. Anal. $C_{18}H_{13}N_3O_2S$ (C, H, N).

4.1.12.5. 1-(Phenylsulfonyl)-3-(thiophen-3-yl)-1*H*-pyrrolo[2,3-*b*]pyridine (20e). Yield = 68%; mp = 164-167 °C (EtOH). ^{1}H NMR ($CDCl_3$-d_1) δ 7.21-7.26 (m, 1H, Ar), 7.35 (dd, 1H, Ar, *J* = 1.2 Hz and *J* = 7.6 Hz), 7.43-7.49 (m, 4H, Ar), 7.57 (t, 1H, Ar, *J* = 7.6 Hz), 7.89 (s, 1H, Ar), 8.09 (dd, 1H, Ar, *J* = 1.2 Hz and *J* = 7.6 Hz), 8.22 (d, 2H, Ar, *J* = 7.6 Hz), 8.47 (dd, 1H, Ar, *J* = 1.2 Hz and *J* = 4.8 Hz). ESI-MS calcd. for $C_{17}H_{12}N_2O_2S_2$, 340.42; found: *m/z* 341.04 $[M + H]^+$. Anal. $C_{17}H_{12}N_2O_2S_2$ (C, H, N).

4.1.13. General procedure for compounds 22a-e

Compounds **22a-e** were obtained starting from **21a-e**[31,22], using m-toluoyl chloride as the reactant, following the same procedure described for compounds **2a-l, 3a-e, 4a,b, 5a-e**. After dilution and neutralization with NaOH, the suspension was extracted with CH_2Cl_2 (3 x 15 mL) and evaporation of the solvent resulted in final compounds **22a-e**, which were purified by column chromatography using hexane/acetone 4:1 (**22c**,**e**) or cyclohexane/ethyl acetate in the following ratios: 1:1 (**22d**), 3:1 (**22b**) and 4:1 (**22a**) as eluents.

4.1.13.1. 3-(1-(3-Methylbenzoyl)-1*H*-pyrrolo[2,3-*b*]pyridin-3-yl)benzonitrile (22a). Yield = 42%; oil. ^{1}H NMR ($CDCl_3$-d_1) δ 2.44 (s, 3H, CH_3), 7.26-7.31 (m, 1H, Ar), 7.39 (t, 1H, Ar, *J* = 7.6 Hz), 7.46 (d, 1H, Ar, *J* = 7.6 Hz), 7.56-7.61 (m, 2H, Ar), 7.63-7.68 (m, 2H, Ar), 7.87 (d, 1H, Ar, *J* = 8.0 Hz), 7.90 (d, 2H, Ar, *J* = 5.6 Hz), 8.14 (d, 1H, Ar, *J* = 7.6 Hz), 8.41 (d, 1H, Ar, *J* = 3.2 Hz). ^{13}C NMR ($CDCl_3$-d_1) δ 21.40 (CH_3), 113.36 (C), 118.09 (C), 118.52 (C), 119.40 (CH), 121.14 (C), 125.07 (CH), 127.47 (CH), 128.12 (CH), 129.94 (CH),

130.67 (CH), 130.82 (CH), 130.98 (CH), 131.76 (CH), 133.53 (C), 133.90 (CH), 134.52 (C), 138.46 (C), 145.46 (CH), 148.76 (C), 167.77 (C). ESI-MS calcd. for $C_{22}H_{15}N_3O$, 337.37; found: *m/z* 338.12 $[M + H]^+$. Anal. $C_{22}H_{15}N_3O$ (C, H, N).

4.1.13.2. (3-(Furan-2-yl)-1*H*-pyrrolo[2,3-*b*]pyridin-1-yl)(m-tolyl)methanone (22b). Yield = 61%; oil. ^{1}H NMR ($CDCl_3$-d_1) δ 2.42 (s, 3H, CH_3), 6.51 (s, 1H, Ar), 6.64 (d, 1H, Ar, *J* = 3.2 Hz), 7.24-7.29 (m, 1H, Ar), 7.36 (t, 1H, Ar, *J* = 7.6 Hz), 7.42 (d, 1H, Ar, *J* = 7.6 Hz), 7.48 (s, 1H, Ar), 7.57 (d, 1H, Ar, *J* = 7.6 Hz), 7.65 (s, 1H, Ar), 7.93 (s, 1H, Ar), 8.26 (d, 1H, Ar, *J* = 8.0 Hz), 8.39 (d, 1H, Ar, *J* = 4.8 Hz). ^{13}C NMR ($CDCl_3$-d_1) δ 21.60 (CH_3), 106.15 (CH), 111.01 (C), 111.47 (CH), 119.37 (CH), 120.29 (C), 122.90 (CH), 127.36 (CH), 127.05 (CH), 129.10 (CH), 130.66 (CH), 133.60 (CH), 133.83 (C), 138.29 (C), 141.83 (CH), 145.31 (CH), 148.17 (C), 148.65 (C), 167.73 (C). ESI-MS calcd. for $C_{19}H_{14}N_2O_2$, 302.33; found: *m/z* 303.11 $[M + H]^+$. Anal. $C_{19}H_{14}N_2O_2$ (C, H, N).

4.1.13.3. (3-(Furan-3-yl)-1*H*-pyrrolo[2,3-*b*]pyridin-1-yl)(m-tolyl)methanone (22c). Yield = 31%; oil. ^{1}H NMR ($CDCl_3$-d_1) δ 2.42 (s, 3H, CH_3), 6.69 (s, 1H, Ar), 7.21-7.26 (m, 1H, Ar), 7.37 (t, 1H, Ar, *J* = 7.2 Hz), 7.43 (d, 1H, Ar, *J* = 7.6 Hz), 7.53 (s, 1H, Ar), 7.57 (d, 1H, Ar, *J* = 7.6 Hz), 7.66 (s, 1H, Ar), 7.80 (s, 1H, Ar), 7.83 (s, 1H, Ar), 8.04 (dd, 1H, Ar, *J* = 1.2 Hz and *J* = 8.0 Hz), 8.36 (d, 1H, Ar, *J* = 4.8 Hz). ^{13}C NMR ($CDCl_3$-d_1) δ 21.39 (CH_3), 109.39 (CH), 111.72 (C), 117.78 (C), 119.18 (CH), 121.79 (C), 123.75 (CH), 127.39 (CH), 127.94 (CH), 128.41 (CH), 130.65 (CH), 133.63 (CH), 134.05 (C), 138.20 (C), 138.95 (CH), 143.70 (CH), 145.10 (CH), 148.83 (C), 167.95 (C). ESI-MS calcd. for $C_{19}H_{14}N_2O_2$, 302.33; found: *m/z* 303.11 $[M + H]^+$. Anal. $C_{19}H_{14}N_2O_2$ (C, H, N).

4.1.13.4. (3-(Pyridin-3-yl)-1*H*-pyrrolo[2,3-*b*]pyridin-1-yl)(m-tolyl)methanone (22d). Yield = 43%; oil. ^{1}H NMR ($CDCl_3$-d_1) δ 2.44 (s, 3H, CH_3), 7.25-7.32 (m, 1H, Ar), 7.39 (t, 1H, Ar, *J* = 7.6 Hz), 7.44 (t, 2H, Ar, *J* = 7.6 Hz), 7.61 (d, 1H, Ar, *J* = 7.6 Hz), 7.69 (s, 1H, Ar), 7.91 (s, 1H, Ar), 7.97 (d, 1H, Ar, *J* = 8.0 Hz), 8.15 (dd, 1H, Ar, *J* = 1.2 Hz and *J* = 8.0 Hz), 8.40 (d, 1H, Ar, *J* = 4.4 Hz), 8.63 (d, 1H, Ar, *J* = 4.0 Hz), 8.87 (s, 1H, Ar). ^{13}C NMR ($CDCl_3$-d_1) δ 21.54 (CH_3), 116.71 (C), 119.51 (CH), 121.37 (C), 124.10 (CH), 124.96 (CH),

127.47 (CH), 128.19 (CH), 128.33 (CH), 129.34 (C), 130.77 (CH), 132.90 (CH), 133.57 (C), 133.86 (CH), 135.00 (CH), 138.30 (C), 145.48 (CH), 148.13 (CH), 148.92 (C), 167.99 (C). ESI-MS calcd. for $C_{20}H_{15}N_3O$, 313.35; found: *m/z* 314.12 $[M + H]^+$. Anal. $C_{20}H_{15}N_3O$ (C, H, N).

4.1.13.5. (3-(Thiophen-3-yl)-1*H*-pyrrolo[2,3-*b*]pyridin-1-yl)(m-tolyl)methanone (22e). Yield = 55%; oil. ^{1}H NMR ($CDCl_3$-d_1) δ 2.42 (s, 3H, CH_3), 7.22-7.28 (m, 1H, Ar), 7.34-7.39 (m, 2H, Ar), 7.41-7.46 (m, 2H, Ar), 7.52 (s, 1H, Ar), 7.58 (d, 1H, Ar, *J* = 7.2 Hz), 7.67 (s, 1H, Ar), 7.84 (s, 1H, Ar), 8.17 (dd, 1H, Ar, *J* = 1.6 Hz and *J* = 8.0 Hz), 8.38 (dd, 1H, Ar, *J* = 1.6 Hz and *J* = 4.8 Hz). ^{13}C NMR ($CDCl_3$-d_1) δ 21.54 (CH_3), 115.54 (C), 119.29 (CH), 121.09 (CH), 121.88 (C), 124.05 (CH), 126.53 (CH), 126.74 (CH), 127.48 (CH), 128.06 (CH), 128.59 (CH), 130.70 (CH), 133.34 (C), 133.61 (CH), 133.98 (C), 138.26 (C), 145.02 (CH), 148.77 (C), 167.94 (C). ESI-MS calcd. for $C_{19}H_{14}N_2OS$, 318.39; found: *m/z* 319.19 $[M + H]^+$. Anal. $C_{19}H_{14}N_2OS$ (C, H, N).

4.2. Biology

4.2.1. HNE inhibition assay

Compounds were dissolved in 100% DMSO at 5 mM stock concentrations. The final concentration of DMSO in the reactions was 1%, and this level of DMSO had no effect on enzyme activity. The HNE inhibition assay was performed in black flat-bottom 96-well microtiter plates. Briefly, a buffer solution containing 200 mM Tris–HCl, pH 7.5, 0.01% bovine serum albumin, 0.05% Tween-20, and 20 mU/mL HNE (Calbiochem) was added to wells containing different concentrations of each compound (up to 50 μM). The most potent HNE inhibitors we tested over a range of 2-400 nM (see **Figure 6**). Reactions were initiated by addition of elastase substrate (N-methylsuccinyl-Ala-Ala-Pro-Val-7-amino-4-methylcoumarin, Calbiochem) in a final reaction volume of 100 μL/well (25 μM final substrate concentration). Kinetic measurements were obtained every 30 s for 10 min at 25 °C using a Fluoroskan Ascent FL fluorescence microplate reader (Thermo Electron, MA) with excitation and emission wavelengths at 355 and 460 nm, respectively. For all compounds

tested, the concentration of inhibitor that caused 50% inhibition of the enzymatic reaction (IC_{50}) was calculated by plotting % inhibition versus logarithm of inhibitor concentration (at least six points). The data are presented as the mean values of at least three independent experiments with relative standard deviations of <15%. Elastase inhibitors Sivelestat and BAE-678 were obtained from Tocris Bioscience (Ellisville, MO) and used as positive controls. For selected lead compounds, inhibition constant (K_i) values were determined using Dixon plots of three to four different concentrations of the substrate[36]. At each substrate concentration, rates were determined with four to five different inhibitor concentrations, and the inverse of the velocities was plotted against the final inhibitor concentration. K_i was determined from the intersection of the plotted lines

4.2.2. Analysis of compound stability

Spontaneous hydrolysis of selected derivatives was evaluated at 25 °C in 0.05 M phosphate buffer, pH 7.3. Kinetics of hydrolysis were monitored by measuring changes in the absorbance spectra over time using a SpectraMax Plus microplate spectrophotometer (Molecular Devices, Sunnyvale, CA). Absorbance (A_t) at the characteristic absorption maxima for each compound was measured at the indicated times until no further absorbance decreases occurred (A_∞) [37]. Using these measurements, we created semilogarithmic plots of $\log(A_t - A_\infty)$ versus time, and k' values were determined from the slopes of these plots. Half-conversion times were calculated using $t_{1/2} = 0.693/k'$, as described previously[19].

4.2.3. Molecular modeling

Initial molecular geometries of the compounds were generated with ChemOffice Professional (Perkin Elmer, Waltham, MA) and optimized by the semi-empirical PM3 method with HyperChem 8.0 (Shimadzu Corporation, Kyoto, Japan). Docking of the molecules was performed using Molegro Virtual Docker (MVD), version 4.2.0 (CLC Bio, Copenhagen, Denmark), as described previously[15]. The structure of HNE co-crystallized with a peptide chloromethyl ketone inhibitor[35] was used for the docking study (1HNE entry of the Protein Data Bank). Docking poses were searched within a sphere of 10 Å radius centered at

the nitrogen atom in the five-membered ring of the peptide chloromethyl ketone inhibitor. This peptide and co-crystallized water molecules were removed from the program workspace, and side chain flexibility was set for the 42 residues closest to the center of the sphere[15]. Fifteen docking runs were performed for each compound, with full flexibility of a ligand around all rotatable bonds and side chain flexibility of the above-mentioned residues of the enzyme. The docking poses with the lowest docking score of each toluoyl derivative were evaluated for the ability to form a Michaelis complex between the hydroxyl group of Ser195 and the carbonyl group in the amido moiety of a docked molecule. For this purpose, values of d_1 [distance O (Ser195) ··C between the Ser195 hydroxyl oxygen atom and the ligand carbonyl carbon atom closest to O(Ser195)] and α [angle O(Ser195)···C=O, where C=O is the carbonyl group of a ligand closest to O(Ser195)] were determined for each docked compound[38]. In addition, the possibility of proton transfer from Ser195 to Asp102 through His57 (the key catalytic triad of serine proteases) was estimated by calculating distances d_2 between the NH hydrogen in His57 and carboxyl oxygen atoms in Asp102, as described previously[15]. The distance between the OH proton in Ser195 and the pyridine-type nitrogen in His57 is also important for proton transfer. However, because of easy rotation of the hydroxyl about the C–O bond in Ser195, we measured distance d_3 between the oxygen in Ser195 and the basic nitrogen atom in His57. The effective length L of the proton transfer channel was calculated as $L = d_3 + \min(d_2)$.

Acknowledgements

This research was supported in part by National Institutes of Health IDeA Program COBRE Grant GM110732; United States Department of Agriculture National Institute of Food and Agriculture Hatch project 1009546; Russian Federation Ministry of Education and Science project 4.6660.2017/8.9; Tomsk Polytechnic University Competitiveness Enhancement Program Grant CEP - N. Kizhner Center - 213/2018; and the Montana State University Agricultural Experiment Station.

References

1. Hashimoto S, Okayama Y, Shime N, Kimura A, Funakoshi Y , Kawabata K , Ishizaka A. Neutrophil elastase activity in acute lung injury and respiratory distress syndrome. *Respirology* **2008**;*13(4)*:581-584.
2. Inoue Y, Seiyama A, Tanaka H, Ukai I, Akimau P, Nishino M, Shimazu T, Sugimoto H. Protective effects of a selective neutrophil elastase inhibitor (sivelestat) on lipopolysaccaride-induced acute dysfunction of the pulmonary microcirculation. *Crit. Care Med.* **2005**;*33(8)*:1814-1822.
3. Pham CT. Neutrophil serine protease: specific regulators of inflammation. *Nat. Rev. Immunol.* **2006**;*6*:541-550.
4. Moroy G, Alix AJ, Sapi J, Hornebeck W, Bourguet E. Neutrophil elastase as a target in lung cancer. *Anticancer Agents Med. Chem.* **2012**;*12*:565-579.
5. Hornebeck W, Robinet A, Duca L, Antonicelli F, Wallach J, Bellon, G. The elastin connection and melanoma progression. *Anticancer Res*. **2005**;*25(4)*:2617-2625.
6. Hilbert N, Schiller J, Arnold J, Arnold K. Cartilage degradation by stimulated human neutrophils: elastase is mainly responsible for cartilage damage. *Bioorg. Chem.* **2002**;*30*:119-132.
7. Von Nussbaum F, Li VMJ. Neutrophil elastase inhibitors for the treatment of (cardio) pulmonary disease: Into clinical testing with pre-adaptive pharmacophores. *Bioorg. Med. Chem. Lett.* **2015**;*25*:4370-4381.
8. Von Nussbaum F, Volkhart ML, Meibom D, Anlauf S, Bechem M, Delbeck M, Gerisch M, Harrenga A, Karthaus D, Lang D, Lustig K, Mittendorf J, Schäfer M, Schäfer S, Schamberger J. Potent and selective human neutrophil elastase inhibitors with novel equatorial ring topology: in vivo efficacy of the polar pyrimidopyridazine BAY-8040 in a pulmonary arterial hypertension rat model. *ChemMedChem* **2016**;*11*:199-206.
9. Armani E, Capaldi C, Sutton JM, Heald RA. Novel compounds. PCT Appl. US 2015/0353561 Al, **2015**.

10. Iwata K, Doi A, Ohji G, Oka H, Oba Y, Takimoto K, Igarashi W, Gremillion DH, Shimada T. Effect of neutrophil elastase inhibitors (sivelestat sodium) in the treatment of acute lung injury (ALI) and acute respiratory distress (ARDS): a systematic review and meta-analysis. *Intern. Med.* **2010**;*49*:2423-2432.
11. Bayer Corp: Prolastin. Company World Wide Web Site. **2002**. http://www.bayerdirect.com/pro.htm/.
12. Vogelmeier C, Aquino TO, O'Brien CD, Perrett J, Gunawardena KA. A randomised, placebo-controlled, dose-finding study of AZD9668, an oral inhibitor of neutrophil elastase, in patients with chronic obstructive pulmonary disease treated with tiotropium. *COPD-J Chron. Obstruct. Pulmon. Dis.* **2012**;*9*:111-120.
13. Von Nussbaum F, Volkhart MJ, Allerheiligen S, Anlauf S, Bärfacker L, Bechem M, Delbeck M, Fitzgerald MF, Gerisch M, Gielen-Haertwig H, Haning H, Karthaus D, Lang D, Lustig K, Meibom D, Mittendorf J, Rosentreter U, Schäfer M, Schäfer S, Schamberger J, Telan AL, Tersteegen A. Freezing the bioactive conformation to boost potency: The Identification of BAY-85-8501, a Selective and Potent Inhibitor of Human Neutrophil Elastase for Pulmonary Diseases. *ChemMedChem* **2015**;*10*:1163-1173.
14. Crocetti L, Giovannoni MP, Schepetkin IA, Quinn MT, Khlebnikov AI, Cilibrizzi A, Dal Piaz V, Graziano A, Vergelli C. Design, synthesis and evaluation of N-benzoylindazole derivatives and analogues as inhibitors of human neutrophil elastase. *Bioorg. Med. Chem.* **2011**;*19*:4460-4472.
15. Crocetti L, Schepetkin IA, Cilibrizzi A, Graziano A, Vergelli C, Giomi D, Khlebnikov AI, Quinn MT, Giovannoni MP. Optimization of *N*-benzoylindazole derivatives as inhibitors of human neutrophil elastase. *J. Med. Chem.* **2013**;*56*:6259-6272.
16. Crocetti L, Schepetkin IA, Ciciani G, Giovannoni MP, Guerrini G, Iacovone A, Khlebnikov AI, Kirpotina LN, Quinn MT, Vergelli C. Synthesis and pharmacological

evaluation of indole derivative as deaza analogues of potent human neutrophil elastase inhibitors. *Drug Dev. Res.* **2016**;*77*:285-299.

17. Giovannoni MP, Schepetkin IA, Crocetti L, Ciciani G, Cilibrizzi A, Guerrini G, Khlebnikov AI, Quinn MT, Vergelli C. Cinnoline derivative as human neutrophil elastase inhibitors. *J. Enzyme Inhib. Med. Chem.* **2016**;*31(4)*:628-639.
18. Vergelli C, Schepetkin IA, Crocetti L, Iacovone A, Giovannoni MP, Guerrini G, Khlebnikov AI, Ciattini S, Ciciani G, Quinn MT. Isoxazol-5(2H)-one: a new scaffold for potent human neutrophil elastase (HNE) inhibitors. *J. Enzyme Inhib. Med. Chem.* **2017**;*32(1)*:821-831.
19. Giovannoni MP, Schepetkin IA, Mark T. Quinn MT, Cantini N, Crocetti L, Gabriella Guerrini G, Iacovone A, Paoli P, Rossi P, Bartolucci G, Menicatti M, Vergelli C. Synthesis, biological evaluation, and molecular modeling studies of potent human neutrophil elastase (HNE) inhibitors. *J. Enzyme Inhib. Med Chem*. **2018**;33(1):1108-1124.
20. Bahekar RH, Jain MR, Jadav PA, Prajapati VM, Patel DN, Gupta AA, Sherma A, Tom R, Bandyopadhya D, Modi H, Patel PR. Synthesis and antidiabetic activity of 2,5-disubstituted-3-imidazol-2-yl-pyrrolo[2,3-b]pyridines and thieno[2,3-b]pyridines. *Org. Proc. Res. Develop.* **2003**;*7(2)*:209-213.
21. Jiang JH, Liu XF, Zhen CH, Zhou YJ, Zho J, Lv JG, Sheng CQ. Acrosin structure-based design, synthesis and biological activities of 7-azaindol derivatives as new acrosin inhibitors. *Chinese Chem. Lett.* **2011**;*22(3)*:272-275.
22. Ibrahim PN, Dean R, Bremer R, Habets G, Mamo S, Nespi M, Zhang C, Zhang J, Zhu YL, Zucherman R, West B, Suzuki Y, Tsai J, Hirm KP, Bollag G, Spevak W, Cho H, Gillette SJ, Wu G, Zho H, Shi S. Pyrrolo[2,3-b]pyridine derivatives as protein kinase inhibitors. *PCT Int Appl.* **2007**, WO 2007002433 A120070104.
23. Minakata S, Hamada T, Komatsu M, Tsuboi H, Kikuta H, Ohshiro Y. Synthesis and biological evaluation of 1H-pyrrolo[2,3-b]pyridine derivatives: correlation between

inhibitory activity against the fungus causing rice blast and ionization potential. *J. Agric. Food Chem.* **1997**;*45*:2345-2348.

24. Baltus CB, Jorda R, Marot C, Berka K, Bazgier V, Krystof V, Priè G, Viaud-Massuard MC. Synthesis, biological evaluation and molecular modeling of a novel series of 7-azaindole based tri-heterocyclic compounds as potent CDK2/Cyclin E inhibitors. *Eur. J. Med. Chem.* **2016**;*108*:701-719.
25. Robinson MM, Robinson BL, Butler FP. 7-Azaindole. VI. Preparation of 5- and 6-substituted 7-azaindoles. *J. Am. Chem. Soc.* **1959**;*81*:743-747.
26. Robison MM, Robison BL. 7-Azandole III. Synthesis of 7-aza analogs of some biologically significant indole derivatives. *J. Am. Chem. Soc.* **1956**;*78*:1247-1251.
27. Chavan NL, Nayak SK, Kusurkar RS. A rapid method toward the synthesis of new substituted tetrahydro α-carbolines and α-carboline. *Tetrahedron* **2010**;*66(10)*:1827-1831.
28. Lape HE, Hoppe JO, Bell MR, Wood D, Selberis WH, Arnold A. Antihypertensive properties of a series of indole and azaindole amidoximes with particular reference to 7-azaindole-3-acetamidoxime. *Arch. Int. Pharmacodyn. Ther.* **1968**;*172(2)*:394-414.
29. Carbone A, Parrino B, Di Vita G, Attanzio A, Spano V, Montalbano A, Baraja P, Tesoriere L, Livrea MA, Diana P, Cirrincione G. Synthesis and antiproliferative activity of thiazolyl-bis-pyrolo[2, 3, c]piridine, nortopsentin analogues. *Marine Drugs* **2015**;*13(1)*:460-492.
30. Zhang J, Ibrahim PN, Bremer R, Spevak W, Cho H. Preparation of azaindole compounds and methods for kinase modulation and indications therefor. *PCT Int Appl.* **2011**, WO 2011057022 A120110512.
31. Lind KE, Cao K, Lin EYS, Nguyen TB, Tangonon BT, Erlanson D, Guekian K, Simmons RL, Lee WC, Sun L, Sting H, Nuzhat P, Lei Z. Preparation of pyridinonyl PDK1 inhibitors. *PCT Int Appl.* **2008**, WO 2008005457 A220080110.

32. Schepetkin IA, Khlebnikov AI, Quinn MT. N-benzoylpyrazoles are novel small-molecule inhibitors of human neutrophil elastase. *J. Med. Chem*. **2007**; *50*:4928–4938.

33. Groutas WC, Kuang R, Venkataraman R, Epp JB, Ruan S, Prakash O. Structure-based design of a general class of mechanism-based inhibitors of the serine proteinases employing a novel amino acid-derived heterocyclic scaffold. *Biochemistry* **1997**;*36:*4739–4750.

34. Vergely I, Laugaa P, Reboud-Ravaux M. Interaction of human leukocyte elastase with a N-aryl azetidinone suicide substrate: conformational analyses based on the mechanism of action of serine proteinases. *J. Mol. Graph.* **1996**;*14(3*):158-167.

35. Navia MA, McKeever BM, Springer JP, et al. Structure of human neutrophil elastase in complex with a peptide chloromethyl ketone inhibitor at 1.84 Å resolution. *Proc. Natl. Acad. Sci. USA* **1989**;*86*:7-11.

36. Dixon M. The determination of enzyme inhibitor constants. *Biochem. J.* **1953**, 55: 170−171.

37. Forist AA, Weber DJ. Kinetics of hydrolysis of hypoglycemic 1-acyl 3,5-dimethylpyrazoles. *J. Pharm. Sci.* **1973**;*62*:318–319.

38. Peters MB and Merz KM. Semiempirical comparative binding energy analysis (SE-COMBINE) of a series of trypsin inhibitors. *J. Chem. Theory Comput.* **2006**;*2*:383-399.

Figures captions

Figure 1. Current HNE inhibitors commercially available or in clinical trials

Figure 2. Design of 7-azaindole (**C**) derivatives based on the indazole (**A**) and indole (**B**) scaffolds of our previous HNE inhibitors.

Figure 3. Inhibition of HNE activity by a representative active 1*H*-pyrrolo[2,3-*b*]pyridine (compound **2b**). HNE was incubated with the indicated concentrations of **2b**, and cleavage of the fluorogenic HNE substrate (25 μM) was monitored. The data are presented as the mean ± S.D. of triplicate samples from a representative experiment of three independent experiments.

Figure 4. Evaluation of HNE inhibition over time by representative 1*H*-pyrrolo[2,3-*b*]pyridines and reference HNE inhibitors, Sivelestat and BAY-678. HNE was incubated with the indicated compounds (5 μM), and kinetic curves monitoring substrate cleavage catalysed by HNE over time are shown. Representative curves are from two independent experiments.

Figure 5. Kinetics of HNE inhibition by compounds **2b** and **5e**. Representative double reciprocal Lineweaver–Burk plots are shown from three independent experiments.
Figure 6. Structures of **CF7**, **FM6**, and **2a**
Figure 7. Docking poses of **2a** and previously published compounds **FM6** and **CF7** in the human neutrophil elastase binding site (1HNE entry of Protein Data Bank[35]). **Panel A**. Docking poses of previously published compounds **FM6** (dark-green) and **CF7** (blue). Co-crystallized ligand peptide chloromethyl ketone is shown in brown. **Panel B**. Docking poses of **FM6** (green) and **2a** (magenta). Hydroxyl oxygen atom of Ser195 is marked by a blue circle. Co-crystallized ligand is shown in brown. Residues within 5 Å from the co-crystallized ligand are visible for both panels.
Figure 8. Superposition of docking poses for compounds **2a** (red), **14** (magenta) and **18** (grey) in the human neutrophil elastase binding site (1HNE entry of Protein Data Bank[35]). Co-crystallized ligand peptide chloromethyl ketone is shown in brown. Residues within 5 Å from this ligand are visible.

1*H*-pyrrolo[2,3-*b*]pyridine: a new scaffold for human neutrophil elastase (HNE) inhibitors

Letizia Crocetti[a], Maria Paola Giovannoni[a]*, Igor A. Schepetkin[b], Mark T. Quinn[b], Andrei I. Khlebnikov[c,d], Niccolò Cantini[a], Gabriella Guerrini[a], Antonella Iacovone[a], Elisabetta Teodori[a], Claudia Vergelli[a]

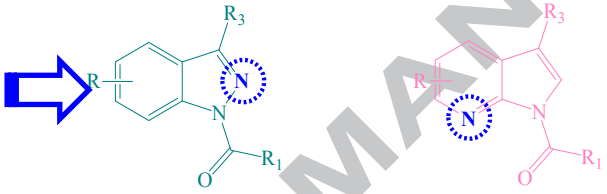

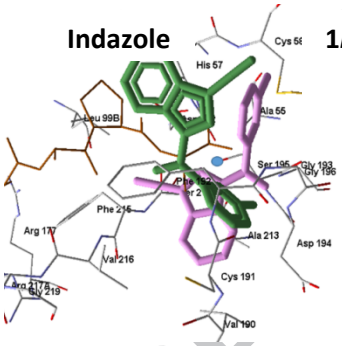

Indazole **1*H*-pyrrolo[2,3-*b*]pyridine**
IC_{50} =14-800 nM